

Geochemistry and Tectonic Environment of Diverse Magma Generations Forming the Crustal Units of the Kızıldağ (Hatay) Ophiolite, Southern Turkey

UTKU BAĞCI¹, OSMAN PARLAK^{2,3} & VOLKER HÖCK⁴

¹ Mersin Üniversitesi, Jeoloji Mühendisliği Bölümü, Çiftlikköy, TR-33342 Mersin, Turkey

² Çukurova Üniversitesi, Jeoloji Mühendisliği Bölümü, Balcalı, TR-01330 Adana, Turkey
(E-mail: parlak@cukurova.edu.tr)

³ Adiyaman Üniversitesi, Mesleki ve Teknik Eğitim Fakültesi, 02040 Adiyaman, Turkey

⁴ University of Salzburg, Department of Geography and Geology, A-5020 Salzburg, Austria

Abstract: The Kızıldağ (Hatay) ophiolite is one of the best preserved Neotethyan oceanic lithospheric remnants in southern Turkey. It is represented by, from bottom to top, mantle tectonites, ultramafic to mafic cumulates, isotropic gabbros, sheeted dike complex, plagiogranites and extrusives (low-K tholeiites and boninites). The ultramafic to mafic cumulate rocks are composed of dunite, wehrlite, olivine gabbro, olivine gabbronorite and gabbro. The crystallization order of cumulus phases, and the presence of highly magnesian olivines and pyroxenes as well as highly calcic plagioclases in the cumulates, indicate a subduction-related tectonic environment and suggest derivation from an island arc tholeiitic magma. The isotropic gabbros are represented by gabbro, diorite and quartz diorite with granular, ophitic to micrographic textures. The sheeted dikes are characterized by diabase and microdiorite with ophitic to intersertal textures. The boninitic volcanics (so-called sakalavites) are basaltic in composition and exhibit hypocrystalline porphyric to hyalopilitic textures. All these rocks are tholeiitic in composition. New geochemical data presented in this paper from the isotropic gabbros, sheeted dikes and sakalavites suggest that there are two main types of parental basic magmas that form the crustal rocks of the Kızıldağ (Hatay) ophiolite. These are (i) IAT series comprising the Group I isotropic gabbros and sheeted dikes; (ii) Low-Ti boninitic series characterized by the Group II isotropic gabbros, sheeted dikes and sakalavites. The spatial and temporal relations of the IAT and boninitic magma types in the Kızıldağ ophiolite indicate that different magma sources were contemporaneously active in a fore-arc tectonic setting of the southern branch of Neotethys during the Late Cretaceous.

Key Words: suprasubduction zone, island arc tholeiite, boninite, fore-arc, Turkey

Kızıldağ (Hatay) Ofiyolitindeki Kabuk Birimlerini Oluşturan Farklı Magma Gelişimlerinin Jeokimyası ve Tektonik Ortamı, Güney Türkiye

Özet: Kızıldağ (Hatay) ofiyoliti, güney Türkiye'de en iyi korunmuş Neotetis okyanusal litosfer kalıntılarından birisi olup tabanlı tavana doğru manto tektonitleri, ultramafik-mafik kümülatlar, izotrop gabrolar, levha dayk kompleksi, plajiyogranitler ve volkaniklerle (düşük-K toleyitler ve boninitler) temsil edilmektedir. Ultramafik ve mafik kümülatlar dunit, verlit, olivinli gabbro, olivinli gabbronorit ve gabro'dan oluşmaktadır. Kümülüks fazların kristalleşme sırasında, kümülatlardaki yüksek-Mg'lu olivin ve piroksenlerin varlığı ve yüksek-Ca'lu plajiyoklaslar dalma-batma ile ilişkili bir tektonik ortamı işaret etmektedir, bu kayaçların adayı toleyitik magmasından türediğini önermektedir. Izotropik gabrolar ofitik-mikrografik doku sunan gabro, diorit ve kuvarslı diyoritler ile temsil edilmektedir. Levha daykları ise ofitik-intersertal dokulu olup diyabaz ve mikrodiorit'lerden oluşmaktadır. Sakalavitler olarak isimlendirilen boninitik volkanikler bazaltik karakterli olup hypokristalen porfirik ve hyalopilitik doku sergilemektedir. Izotropik gabrolar, levha daykları ve sakalavitlerden elde edilen yeni jeokimyasal veriler Kızıldağ (Hatay) ofiyolitinde okyanusal kabuk kayaçlarını oluşturan iki ana magmanın varlığına işaret etmektedir. Bunlar: (i) Grup I, izotrop gabro ve levha dayklarını oluşturan adayı toleyitik serisi ve (ii) Grup II, izotrop gabrolar, levha daykları ve sakalavitleri oluşturan düşük-Ti boninitik seridir. Kızıldağ ofiyolitindeki boninitik ve ada yayı toleyitik magmatizmasının mekansal ve zamansal ilişkileri, farklı magma kaynaklarının Geç Kretase'de Neotetis okyanusunun güney kolundaki yay-önü tektonik ortamında eşzamanlı olarak aktif olduklarını işaret etmektedir.

Anahtar Sözcükler: dalma-batma zonu üstü, ada yayı toleyiti, boninit, yay-önü, Türkiye

Introduction

Suprasubduction zone tectonic settings include island arcs, fore-arc and back-arc basins for the generation of oceanic crust (ophiolite). Suprasubductional ophiolites (cf. Pearce *et al.* 1984) often contain a geochemical stratigraphy which includes island arc tholeiites (IAT), boninitic series volcanics as well as lavas transitional between IAT and mid-ocean ridge basalts (MORB) (Beccaluva *et al.* 1984, 2004, 2005; Malpas & Langdon 1984; Beccaluva & Serri 1988; Smellie *et al.* 1995; Meffre *et al.* 1996; Parlak 1996; Bedard *et al.* 1998; Bedard 1999; Parlak *et al.* 2000; Dilek & Flower 2003; Pearce 2003; Pe-Piper *et al.* 2004; Saccani & Photiades 2004, 2005; Rızaoglu *et al.* 2006).

The Anatolian segment of the Alpine-Himalayan orogen comprises remnants of Neotethyan oceanic basins cropping out along E-W-trending tectonic zones between metamorphic massifs and/or platform carbonates (Şengör & Yılmaz 1981; Dilek *et al.* 1999; Robertson 2002) (Figure 1). The remnants of Neotethys, in a structurally descending order, are characterized by ophiolites,

metamorphic soles and ophiolitic mélanges. These ophiolites and related subduction-accretion units were generated during the closing stages of the Neotethyan oceanic basins in the Late Cretaceous (Dilek & Flower 2003). Well-preserved Neotethyan ophiolites in Turkey are of supra-subduction zone (SSZ) type (Parlak *et al.* 1996, 2000, 2002; Yalınız *et al.* 1996; Robertson 2002; Bağci *et al.* 2005, 2006) and display a consistent sequence of events during their formation and emplacement.

The Kızıldağ (Hatay) ophiolite is situated in the peri-Arabian ophiolite belt that includes the Troodos (Cyprus) and Semail (Oman) ophiolites (Figure 1), which have been important in the evolution of ideas concerning the origin and significance of ophiolites and ophiolite-ocean crust analogy (Moores & Vine 1971; Gass & Smewing 1973; Panayiotou 1980; Coleman 1981; Lippard *et al.* 1986; Nicolas 1989; Dilek *et al.* 1990; Malpas *et al.* 1990; Dilek & Delaloye 1992; Dilek & Eddy 1992; Dilek & Thy 1998; Dilek 2003). Investigations in the Kızıldağ (Hatay) ophiolite covered seafloor spreading tectonics and

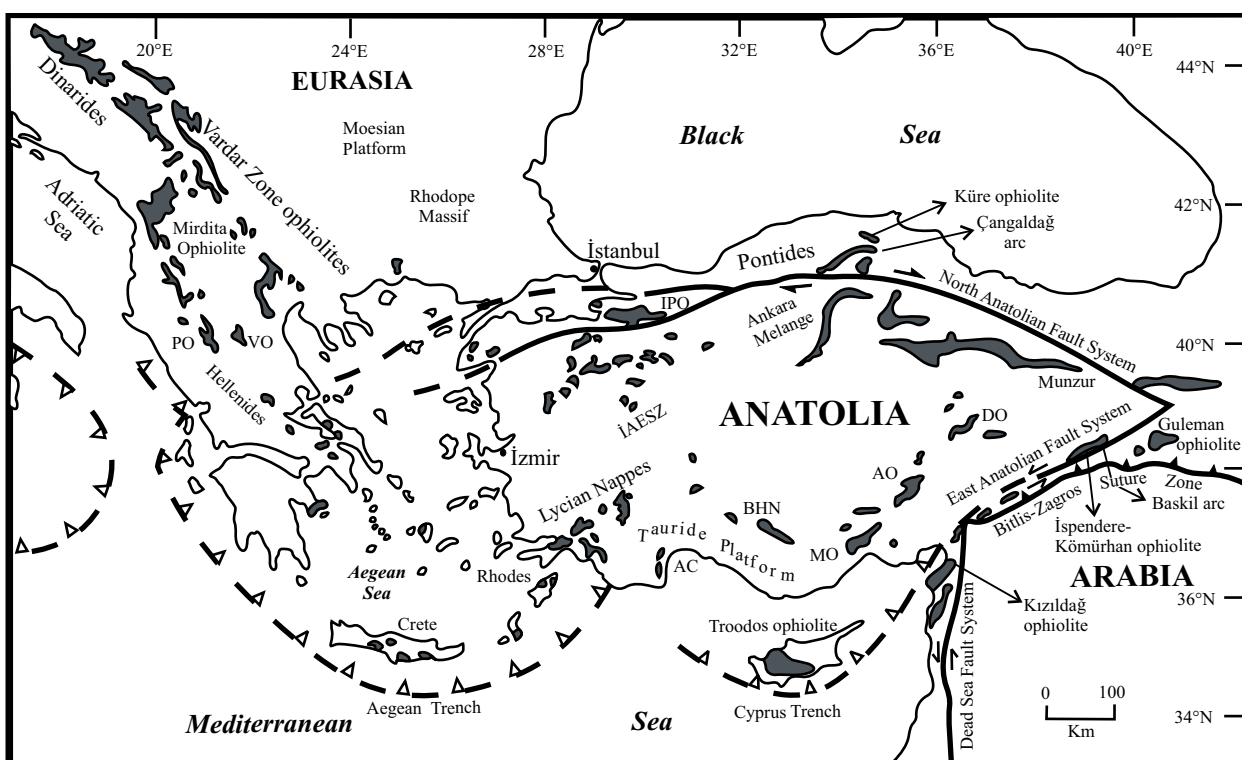


Figure 1. Distribution of Neotethyan ophiolites and major tectonic features in the eastern Mediterranean region (from Dilek & Flower 2003). AC- Antalya Complex; IPO- Intra Pontide Ophiolites; BHN- Beyşehir-Hoyran Nappes; İAESZ- İzmir-Ankara-Erzincan Suture Zone; MO- Mersin Ophiolite; PO- Pindos Ophiolite; VO- Vourinos Ophiolite; AO- Aladağ Ophiolite; DO- Divriği Ophiolite.

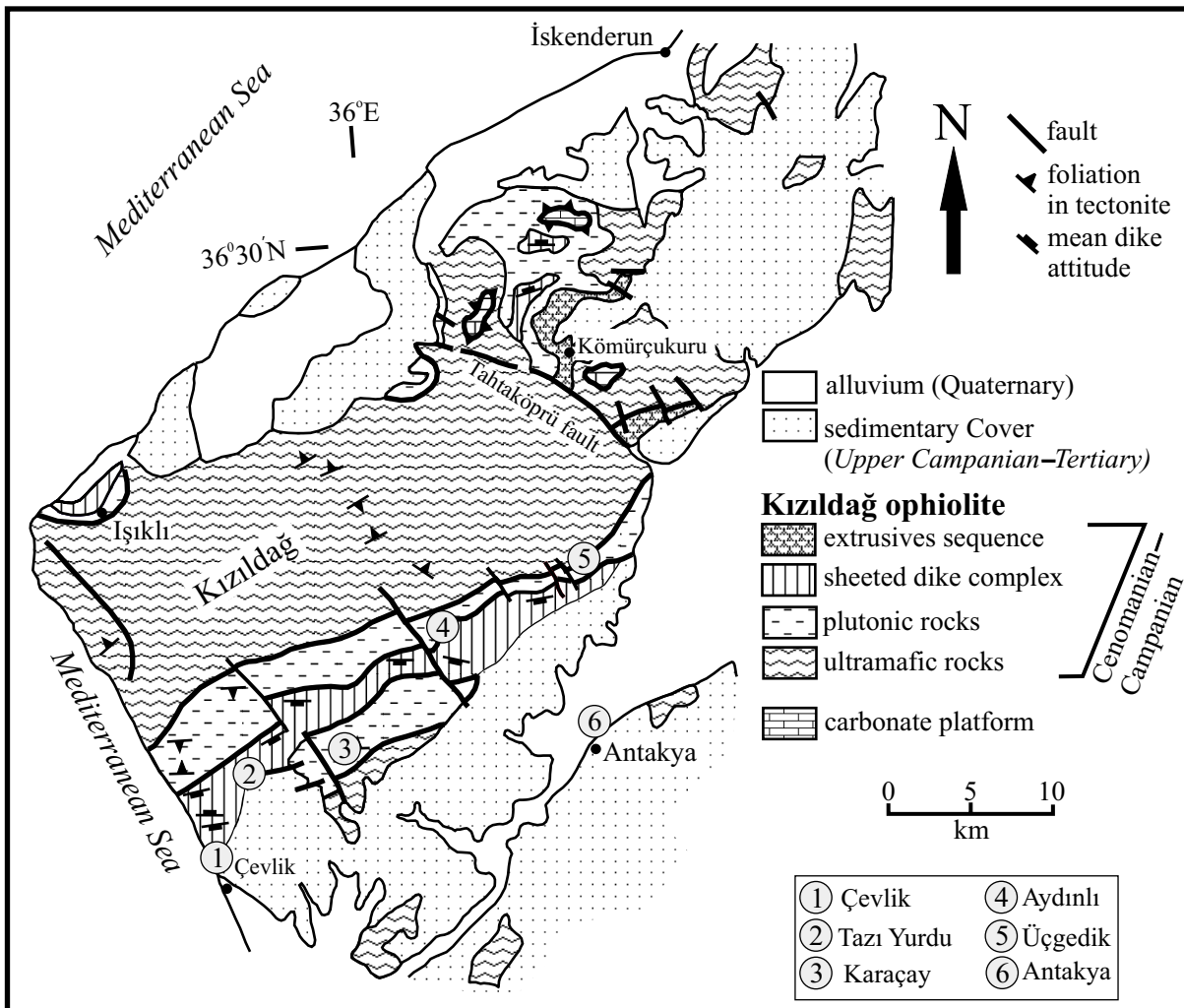


Figure 2. Geological map of the Kızıldağ ophiolite (from Selçuk 1981; Tekeli & Erendil 1984; Dilek & Thy 1998).

structure of oceanic crust as well as petrology of the plutonic and extrusive rocks (Dilek & Delaloye 1992; Dilek & Eddy 1992; Lytwyn & Casey 1993; Dilek & Thy 1998; Bağci *et al.* 2005). Lytwyn & Casey (1993) showed the existence of boninites and island arc tholeiites from the volcanics and sheeted dikes of the Kızıldağ (Hatay) ophiolite and suggested that the Troodos and Kızıldağ (Hatay) ophiolites may be petrogenetically and tectonically related.

In this paper, new geochemical data from the isotropic gabbros and sakalavites (cf. Dubertret 1955), and complementary geochemical data for the sheeted dikes will be presented in order to demonstrate (a) the generation of voluminous boninitic and island arc

tholeiitic (IAT) magmatism that formed different parts of the oceanic crust (Kızıldağ ophiolite) during the development of the Late Cretaceous subduction/accretion system in southern Neotethys, (b) spatial and temporal interaction of these magmatic suites, and (c) to compare our results with those from other eastern Mediterranean ophiolites and modern analogues.

Regional Geology

The Kızıldağ ophiolite (Figure 2) in southern Turkey is 25 km wide, 45 km long, up to 7 km thick and covers an area of approximately 950 km² (Figure 2) (Tinkler *et al.* 1981; Tekeli *et al.* 1983). The Kızıldağ ophiolite thrust

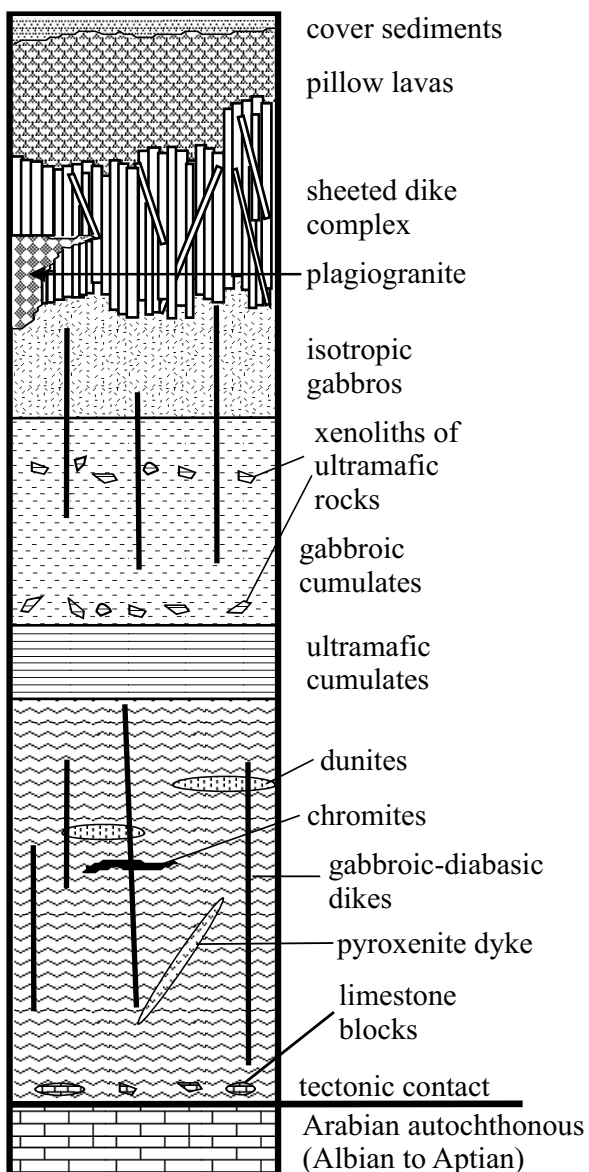


Figure 3. Synthetic log of the Kızıldağ (Hatay) ophiolite (not to scale).

sheets rest tectonically on the top of Arabian platform carbonates that are Early Cretaceous (Albian to Aptian) in age. The oldest transgressive sequence covering the ophiolitic rocks comprises conglomerate, sandstone and neritic to pelagic carbonates (Selçuk 1981; Tinkler *et al.* 1981; Delaloye & Wagner 1984) of Maastrichtian age. Therefore, the emplacement age of the Kızıldağ ophiolite is limited to the Late Cretaceous (pre-Maastrichtian). It displays a complete ophiolite assemblage that comprises, from bottom to top, depleted mantle tectonites,

ultramafic to mafic cumulates, isotropic gabbro, sheeted dikes, plagiogranites and a volcanic complex (Figure 3). The mantle tectonites constitute the core of the ophiolite body and are represented primarily by harzburgite with local lenses and bands of dunite. The base of the serpentized tectonites contains large blocks of limestones (10–20 m thick and 20–40 m long) near Kömürçukuru (Figures 2 & 3), which were incorporated into the peridotite during the emplacement of the ophiolite (Tinkler *et al.* 1981). The harzburgitic tectonites exceed 3 km in thickness and are intruded by pegmatitic gabbroic and pyroxenitic dikes (Figure 4a, b) (Tinkler *et al.* 1981; Tekeli *et al.* 1983; Erendil 1984; Dilek & Thy 1998). The cumulate rocks displaying a thickness from 165 to 700 m, are characterized by dunite, wehrlite, olivine gabbro, olivine gabbronorite and gabbro (Figure 4c). Near the top of the plutonic section, isotropic gabbros are more abundant, with a thickness of 2–2.5 km (Tinkler *et al.* 1981; Pişkin *et al.* 1990). They are represented by gabbro, diorite and quartz diorite rock assemblages. At the top, the isotropic gabbros grade into a well-developed sheeted dike complex containing several gabbro screens and lenses 50 to 70 cm in size (Erendil 1984; Tinkler *et al.* 1981; Dilek & Thy 1998) at the base (Figure 4d). The sheeted dikes start as isolated dikes at the basal contact with the isotropic gabbro, and are dominated by 100% dikes ranging in thickness from 2 cm to 2 meters. The best-preserved outcrops were observed north of Çevlik along the Mediterranean coastline. Some small outcrops of the sheeted dike complex are seen north of Kömürçukuru and Tahtaköprü (Figure 2). The sheeted dikes are oriented along a strike of E–W and display well-preserved chilled margins and cross-cutting relationships. Dilek & Thy (1998), based on cross-cutting relations, textural and compositional differences, showed that at least three main generations of dike intrusions exist in the sheeted dike complex (Figure 4e, f). The plagiogranite has an intrusive relationship with the upper part of the isotropic gabbros in the Karaçay valley and the sheeted dike complex in Çevlik village (Figure 4g). Two outcrops of the volcanic rocks are present in the Kızıldağ ophiolite. The first one is located in two areas, at or near Tahtaköprü and Kömürçukuru villages in the northern part of the massif (Figure 2). They tectonically overlie serpentized peridotite in Tahtaköprü and isotropic gabbro in Kömürçukuru, respectively (Dilek & Thy 1998). The

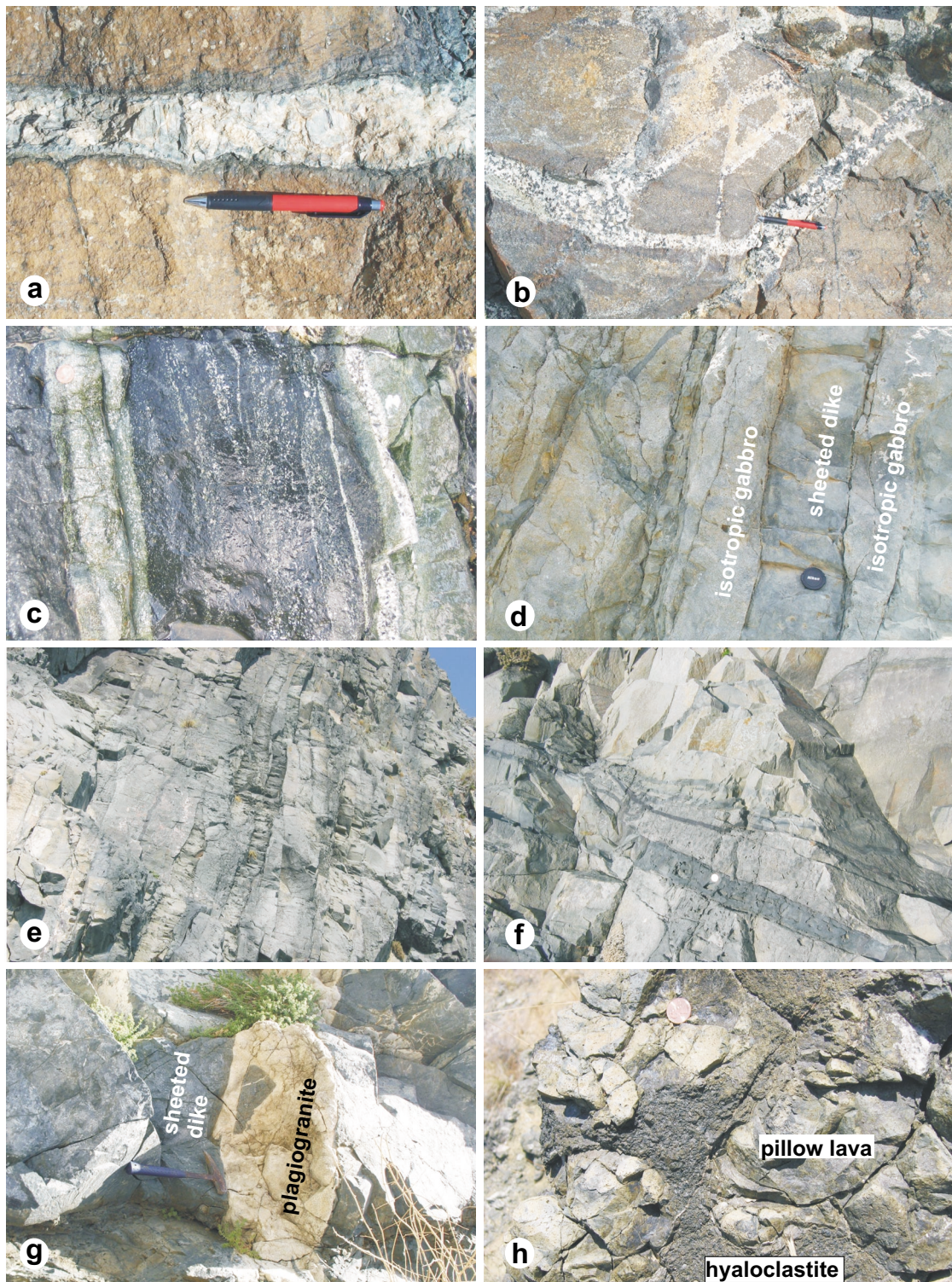


Figure 4. Field views of the crustal rocks from the Kızıldağ (Hatay) ophiolite: (a) Pyroxenite dike in harzburgite; (b) pegmatitic gabbro veinlet in harzburgite; (c) ductilely deformed cumulate rocks; (d) isotropic gabbro-sheeted dike transition near Çevlik; (e, f) parallel to sub-parallel sheeted dikes and cross-cutting relations; (g) plagiogranite intruding the sheeted dikes and (h) pillow lavas surrounded by hyaloclastites in boninites. Pencil and hammer are 11 and 33 cm long, respectively. The coin and lense cap have diameters of 2.5 and 5.8 cm, respectively.

volcanic complex consists of pillow basalts, massive lavas and cross-cutting dikes and is 1.3 km thick, with an outcrop area of 5 km² (Tekeli *et al.* 1983; Erendil 1984). The lavas are interbedded with metalliferous umbers (Robertson 1986a). The second group of volcanic rocks is located 12 km southeast of the main body of the Kızıldağ ophiolite near Mount Silpius and is referred to as 'sakalavite' by Dubertret (1955). It is 300 m thick and represented by hyaloclastites associated with boninitic egg-shaped micro pillow lavas, 4–5 cm to 20 cm long (Laurent *et al.* 1980; Robertson 1986b) (Figure 4h).

Petrography and Mineralogy

This section only summarizes the petrographic characteristics of the studied rocks because those of other rock units in the Kızıldağ (Hatay) ophiolite were already given elsewhere (Bağcı *et al.* 2005).

The boninitic volcanic rocks in the Kızıldağ (Hatay) ophiolite are called sakalavites (cf. Dubertret 1955). They exhibit hypocrystalline porphyric to hyalopilitic texture and are characterized by olivine (20 vol%), clinopyroxene (60–65 vol%), plagioclase (1–5 vol%) and chromite (1–3 vol%) in a glassy groundmass. Glass between the phenocrysts and pillows has been altered to montmorillonite or partly recrystallized to palagonite (Laurent *et al.* 1980). The olivine forms euhedral to subhedral phenocrysts up to 1.28 mm long. Occasionally completely fresh, they more often occur as skeletal forms (Figure 5a, b). Serpentine and iddingsite are the secondary phases. The olivine compositions were obtained by microprobe analyses and are presented in Table 1. The olivines are markedly less magnesian, varying from Fo_{87.5} to Fo_{89.5}, than those from the mantle tectonite (Pişkin *et al.* 1990). A slight difference in Mg and Fe contents between the core and rim of individual grains is observed (Table 1). These values are similar to olivines from the ultramafic cumulates (Bağcı *et al.* 2005) and fall within the range of boninitic olivines from Troodos ophiolite Upper Pillow Lavas (Malpas & Langdon 1984), and Mariana trench boninites (Bloomer & Hawkins 1987). The clinopyroxenes differ texturally from olivines because the grains have developed forms and shapes indicative of rapid quenching (Figure 5c, d). They display stubby, swallow-tail and hourglass forms, ranging from 0.01 to 0.6 mm in length (Figure 5c, d). The clinopyroxene compositions were obtained by microprobe analyses and are presented in Table 1. They

are mainly calcic to subcalcic augite (Wo_{44–18}, En_{69–34}, Fs_{29–7}) in composition. They exhibit zoning, and have Mg-rich cores and Al₂O₃-, FeO- and CaO-rich rims (Table 1). The Ca-rich plagioclase (An₈₃) is represented by anhedral grains (0.05–0.18 mm) (Laurent *et al.* 1980). The chromite microphenocrysts, which are generally surrounded by olivine, occur as euhedral grains and have high Cr# (Cr/Cr+Al= 70) (Table 1), which is also typical of those found in boninites (Crawford *et al.* 1989).

The parallel- to subparallel-oriented dikes are dominated by diabase and quartz-microdiorite. The diabase exhibits intersertal, ophitic to subophitic textures (Figure 5e, f) and is characterized by euhedral to subhedral plagioclase (60–70 vol%) with a grain size of 0.03 to 0.9 mm, anhedral clinopyroxene (20–25 vol%) with a grain size of 0.18 to 2.17 mm and opaque minerals. The quartz microdiorite displays microgranular porphyric texture (Figure 5e, f) and is represented by subhedral plagioclase (An_{40–50}) (60–70 vol%) with a grain size of 0.15 to 2.1 mm, anhedral hornblende (15–20 vol%) with a grain size of 0.03 to 0.53 mm, anhedral quartz (5–10 vol%) with a grain size of 0.01 to 0.18 mm and opaque minerals. Epidote and chlorite are present as secondary phases.

The isotropic gabbros form the uppermost part of the plutonic section and are 2000 meters thick. They have transitional contacts with the cumulate rocks in the Çevlik, Karaçay, Aydınlı and Üçgedik regions (Figure 2). They exhibit light brown to green weathered surfaces and deep green to green fresh surfaces. The isotropic gabbroic rocks of the Kızıldağ (Hatay) ophiolite consist of gabbro, diorite and quartz diorite. The gabbro displays granular to ophitic textures (Figure 5g, h) and is characterized by prismatic plagioclase (55–60 vol%) with a grain size of 0.3 to 1.9 mm, subhedral clinopyroxene (30 vol%) with a grain size of 0.5 to 2.3 mm and opaque minerals. The diorite exhibits granular, ophitic to subophitic texture and is represented by euhedral to subhedral plagioclase (80 vol%) with a grain size of 0.4 to 1.6 mm, subhedral hornblende (10–15 vol%) with a grain size of 0.4 to 1.2 mm, clinopyroxene (1–5 vol%) and opaque minerals. The quartz diorite displays granular, ophitic and micrographic textures (Figure 5g, h). It consists of plagioclase laths (andesine) (60–70 vol%) with a grain size of 0.4 to 1.3 mm, subhedral to anhedral hornblende (15–20 vol%) with a grain size of 0.6 to 1.8 mm, anhedral clinopyroxene (~ 5 vol%) with

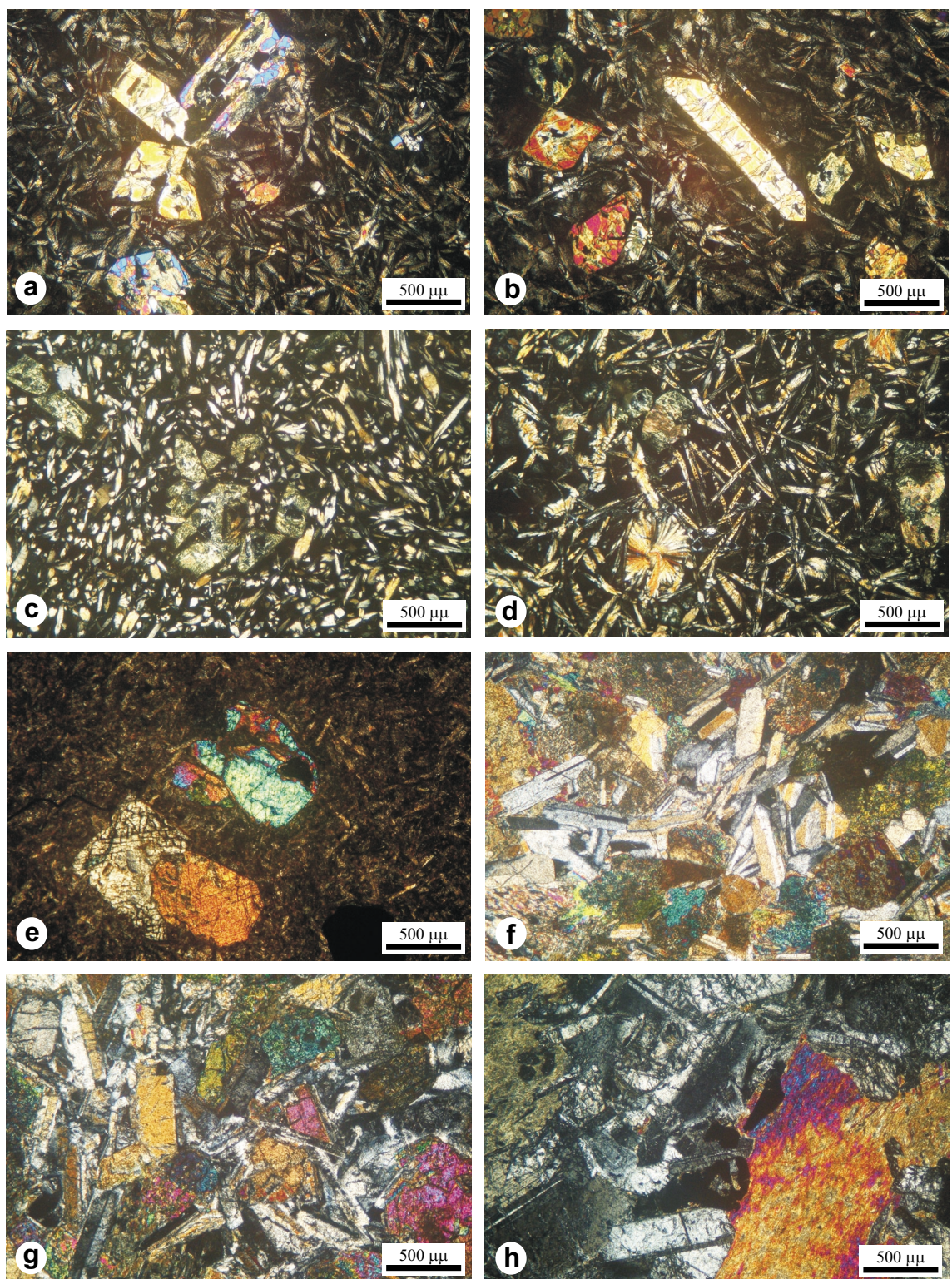


Figure 5. Petrographic views of the crustal rocks from the Kizildağ (Hatay) ophiolite: (a, b) skeletal forms of the olivines in boninites; (c, d) stubby, swallowtail and hourglass shapes indicating of rapid quenching in boninitic lava; (e, f) microgranular to subophitic textures in sheeted dikes; (g, h) ophitic to granular textures in isotropic gabbros.

Table 1. Representative mineral chemistry data from the sakalavites in the Kizildağ (Hatay) ophiolite.

Sample	Olivine								Pyroxene								Chromite				
	SKL2-1c	SKL2-8c	SKL2-5c	SKL16-5r	SKL2-1c	SKL2-7c	SKL2-11c	SKL2-14c	SKL14-1c	SKL14-6c	SKL14-6r	SKL14-9c	SKL14-9r	SKL16-5c	SKL16-6r	SKL16-8c	SKL16-11c	SKL16-1c	SKL16-2c		
SiO ₂	40.62	40.43	41.39	41.26	46.40	54.50	52.62	45.56	53.05	54.69	50.47	53.20	51.67	53.78	51.01	49.82	51.93	50.03	0.07	0.07	
TiO ₂	0.00	0.00	0.00	0.00	0.45	0.12	0.17	0.56	0.30	0.18	0.63	0.34	0.40	0.23	0.44	0.38	0.35	0.47	0.32	0.29	
Al ₂ O ₃	0.03	0.04	0.02	0.03	11.66	3.02	3.31	12.56	4.12	2.76	7.19	4.20	5.98	3.69	6.61	8.47	5.79	8.24	15.07	15.25	
Cr ₂ O ₃	0.06	0.08	0.08	0.08	0.02	0.40	0.70	0.05	0.65	1.12	0.05	0.51	0.05	0.65	0.14	0.07	0.12	0.03	50.15	49.28	
FeO*	11.01	11.60	10.00	11.12	10.51	7.51	5.13	9.81	6.31	6.89	7.51	6.11	7.60	6.40	5.76	7.08	6.28	6.25	20.82	20.82	
MnO	0.20	0.17	0.15	0.17	0.27	0.16	0.16	0.20	0.23	0.19	0.18	0.12	0.18	0.20	0.13	0.20	0.15	0.15	0.17	0.24	
MgO	47.63	47.19	47.92	47.00	13.25	24.40	18.07	11.73	19.15	23.53	15.60	18.91	17.01	21.65	15.93	15.52	17.82	14.92	12.39	12.41	
NiO	0.25	0.28	0.28	0.17	0.04	0.04	0.05	0.00	0.03	0.01	0.03	0.01	0.01	0.02	0.03	0.04	0.02	0.01	0.08	0.14	
CaO	0.21	0.20	0.15	0.17	16.63	8.91	19.17	18.87	16.08	10.56	18.24	16.51	16.99	13.31	19.88	18.31	17.45	19.81	0.07	0.08	
Na ₂ O	0.00	0.00	0.00	0.00	0.10	0.09	0.10	0.10	0.05	0.08	0.09	0.05	0.10	0.07	0.06	0.08	0.09	0.08	0.00	0.00	
K ₂ O	0.00	0.00	0.01	0.00	0.00	0.02	0.01	0.00	0.01	0.00	0.01	0.00	0.01	0.00	0.01	0.00	0.00	0.01	0.01	0.01	
Total	100.00	100.00	100.00	100.00	99.33	99.18	99.49	99.44	100.00	100.00	100.00	100.00	100.00	100.00	100.00	100.00	100.00	100.00	99.14	98.60	
Fo	88.52	87.88	89.52	88.28																	
Fa	11.48	12.12	10.48	11.72																	
En					42.40	69.50	51.90	37.95	55.70	67.06	47.24	55.18	50.66	62.00	47.52	47.37	52.46	45.57			
Fs						19.36	12.27	8.53	18.18	10.68	11.32	13.07	10.20	12.99	10.61	9.87	12.47	10.63	10.96		
Wo						38.24	18.23	39.57	43.87	33.62	21.62	39.69	34.62	36.35	27.39	42.61	40.15	36.91	43.46		
Mg#	88.52	87.88	89.52	88.28	69.20	81.73	85.04	68.06	80.16	81.51	75.31	79.53	76.36	82.25	80.01	77.25	80.48	77.44	51.48	51.51	
Cr#																			69.07	68.44	

a grain size of 0.2 to 0.8 mm, anhedral quartz (~10 vol%) and opaque minerals. Chlorite, albite, sericite, kaolinite, actinolite and epidote are the secondary phases in these rocks.

Analytical Method

A total of 67 samples (22 isotropic gabbros, 27 sheeted dykes and 18 boninitic volcanics) were analyzed for major and trace element contents. Major and trace element analyses were carried out at the University of Geneva (Switzerland). Major elements were determined by XRF spectrometry on glass beads fused from ignited powders to which $\text{Li}_2\text{B}_4\text{O}_7$ was added (1:5), in a gold-platinum crucible at 1150 °C. Trace elements were analysed on pressed powder pellets by the same method. A subset of 35 representative samples (14 isotropic gabbros, 15 sheeted dykes and 6 boninitic volcanics) were analysed by ICP-MS for trace elements (including REE) at Acme Analytical Laboratories and Actilabs-Activation Laboratories in Canada. A total of 3 representative polished sections from the boninitic volcanics were selected for electron microprobe analysis on a JEOL JXA-8600 at the Geology and Paleontology Department at Salzburg University (Austria). The analytical conditions for the elements were 13 s (10 s for Peak and 3 s for Background) of counting interval, beam current -20 nA and acceleration voltage -15 kV. The data reduction was done following the ZAF procedure. Fe^{+3} and Fe^{+2} were determined from stoichiometry of spinel using the equation of Droop (1987). The results of the analyses are presented in Tables 1 to 7.

Geochemistry

The major, trace and rare earth element contents of the isotropic gabbro, sheeted dike and boninitic volcanic (sakalavite) rocks are presented in Tables 2 to 7. The LOI values range up to 5.99% in isotropic gabbros, 6.43% in sheeted dikes and 13.38% in boninitic volcanics (sakalavite), reflecting variable secondary alteration indicated by the presence of secondary mineral phases (i.e. serpentine, epidote, kaolin, calcite, chlorite), as determined in the petrography section. The mobility of many elements during low-grade submarine alteration is well constrained (e.g., Hart *et al.* 1974; Humphris & Thompson 1978). For this reason, recourse is generally made to relatively immobile elements such as Ti, P, Zr, Y,

Nb and REE, and to a lesser extent Cr, Ni, Sc and V, to designate rock groups, petrogenetic trends and tectonic environments (Pearce & Cann 1973; Floyd & Winchester 1975; Winchester & Floyd 1977; Pearce & Norry 1979).

The Nb/Y ratios of the isotropic gabbro, sheeted dike, and sakalavite rocks range from 0.05 to 0.33, 0.04 to 0.31 and 0.15 to 0.42, respectively (Tables 2, 4 & 6). These indicate that the analysed rocks are derived from a tholeiitic magma source (Pearce 1982) (Figure 6a). The rock classification diagram for the rock units of the Kızıldağ (Hatay) ophiolite is based on ratio-ratio plot of immobile elements such as Zr/Ti versus Nb/Y (Pearce 1996). All the rocks from the isotropic gabbros, sheeted dikes and sakalavites plot in the basaltic field (Figure 6b).

The variations of some selected major and trace elements are presented in Figure 7. SiO_2 , FeO , Y and V show positive correlations, whereas MgO , $\text{CaO}/\text{Al}_2\text{O}_3$, Cr and Ni exhibit negative correlations against Zr, consistent with a crystallization assemblage of olivine, clinopyroxene and plagioclase (Pearce & Norry 1979; Pearce 1982) (Figure 7). All the interelement relations and immobile trace element contents (Table 2 to 7) suggest that two geochemically distinct subgroups in the isotropic gabbro and two distinct subgroups in the sheeted dikes can be identified. The first geochemical group includes the Group I isotropic gabbros and sheeted dikes while the second group includes the Group II isotropic gabbros, sheeted dikes and sakalavites (Table 2 to 7). The first group is represented by high TiO_2 (0.43–1.06 wt%), Zr (24–54 ppm), Y (15–30 ppm), and V (169–399 ppm) and low MgO (3.88–9.60 wt%), Ni (27–67 ppm), and Cr (20–666 ppm) compared to the second group which is characterized by low TiO_2 (0.19–0.61 wt%), Zr (11–31 ppm), Y (9–23 ppm), and V (136–295 ppm) and high MgO (8.48–16.92 wt%), Ni (64–418 ppm), and Cr (54–1495 ppm) (Tables 2 to 7).

On the $\text{Al}_2\text{O}_3/\text{TiO}_2$ versus TiO_2 plot of the isotropic gabbros, sheeted dikes and sakalavites (Figure 8a), the first geochemical group (Group I isotropic gabbro and sheeted dike) is represented by low $\text{Al}_2\text{O}_3/\text{TiO}_2$ (14.45–34.61) and plots within the transitional field of mid ocean ridge basalt (MORB) and island arc tholeiite (IAT) whereas the second geochemical group has higher $\text{Al}_2\text{O}_3/\text{TiO}_2$ (23.81–83.8) contents and shares chemical affinity with both boninites and IAT (Figure 8a). The Zr versus TiO_2 plot of the isotropic gabbros, sheeted dikes and sakalavites (Figure 8b) shows that the first

Table 2. Major and trace element contents of the isotropic gabbros from the Kızıldağ (Hatay) ophiolite.

Sample	IAT-type isotropic gabbro						Boninitic-type isotropic gabbro															
	K-6	KC-30	KC-34	KC-35	KC-36	KC-39	KC-41	KC-46	Ü-6	T-6	K-8	K-27	K-28	KC-28	KC-32	KC-33	KC-38	KC-40	KC-44	KC-45	KC-48	
S10 _z	51.01	54.60	52.14	57.19	55.96	51.95	45.67	54.28	50.92	52.71	50.09	46.96	47.86	47.92	50.48	49.71	48.51	50.24	46.09	49.46	49.16	46.20
T10 _z	0.54	0.43	0.53	0.93	1.02	0.74	0.56	0.78	0.50	0.92	0.67	0.32	0.21	0.20	0.41	0.31	0.32	0.46	0.37	0.29	0.34	0.19
Al ₂ O ₃	16.31	14.92	16.43	15.23	15.52	16.39	17.82	16.16	16.68	16.12	15.50	16.76	15.18	16.34	14.63	12.63	15.47	13.92	15.79	16.39	16.15	11.45
FeO*	8.37	6.90	7.65	9.65	10.15	9.21	7.38	9.89	6.02	10.18	9.66	5.94	5.00	5.19	7.08	8.44	6.63	9.60	5.63	5.43	6.41	8.96
MnO	0.16	0.11	0.10	0.08	0.08	0.10	0.12	0.13	0.11	0.11	0.10	0.10	0.11	0.11	0.14	0.13	0.12	0.18	0.09	0.11	0.13	0.15
MgO	7.96	8.03	7.86	4.84	5.21	6.81	9.46	5.65	7.86	5.45	7.43	10.51	10.74	9.91	9.52	13.96	10.62	11.20	12.00	9.48	9.40	16.92
CaO	9.02	9.18	10.46	5.60	4.50	10.63	12.04	7.91	11.74	8.19	10.06	13.66	16.67	16.10	10.54	9.82	13.69	9.34	12.44	12.67	13.77	12.03
Na ₂ O	3.53	3.05	2.44	4.06	4.68	2.18	1.13	2.80	2.84	3.95	3.15	1.63	1.10	1.20	2.58	1.30	1.41	1.86	1.38	2.37	1.57	0.38
K ₂ O	0.41	0.19	0.16	0.26	0.43	0.17	0.46	0.48	0.19	0.32	0.18	0.30	0.02	0.03	0.30	0.11	0.09	0.20	0.22	0.25	0.40	0.03
P ₂ O ₅	0.04	0.05	0.04	0.10	0.09	0.05	0.03	0.07	0.05	0.08	0.05	0.03	0.01	0.01	0.02	0.02	0.03	0.01	0.03	0.02	0.03	0.02
Li ₂ O	2.57	2.01	1.55	1.62	2.05	1.18	4.44	1.55	2.44	1.64	2.45	3.20	2.51	2.48	3.45	3.01	1.71	2.54	5.99	2.58	1.98	2.85
Cr ₂ O ₃	0.01	0.09	0.01	0.01	0.01	0.01	0.00	0.02	0.01	0.01	0.08	0.17	0.08	0.08	0.14	0.09	0.03	0.08	0.10	0.08	0.18	
NiO	0.01	0.01	0.01	0.00	0.00	0.00	0.01	0.00	0.01	0.00	0.01	0.02	0.03	0.02	0.05	0.02	0.01	0.02	0.02	0.02	0.07	
Total	99.93	99.57	99.38	99.57	99.69	99.42	99.13	99.70	99.37	99.69	99.35	99.50	99.61	99.57	99.25	99.61	98.71	99.58	99.82	99.17	99.44	99.42
Nb	2	3	2	6	5	2	1	3	1	3	2	1	1	1	2	4	1	3	1	1	1	3
Zr	24	40	32	51	54	37	24	40	31	39	32	18	11	11	16	16	20	23	15	18	20	14
Y	15	23	20	29	30	22	16	25	18	25	19	11	9	9	12	14	12	15	14	13	14	9
Sr	96	72	85	129	125	98	323	96	124	360	123	147	69	76	113	43	49	59	162	51	67	40
U	2	2	2	3	2	3	2	2	2	2	2	2	2	2	2	2	2	2	2	2	2	
Rb	5	4	4	5	5	5	7	6	4	4	6	4	4	4	5	5	4	4	4	4	5	
Th	2	2	2	2	2	2	2	2	2	2	2	2	2	2	2	2	2	2	2	2	2	
Pb	7	9	8	7	6	9	7	10	5	6	8	7	8	8	6	13	9	10	7	4	7	
Ga	14	15	18	18	15	17	19	15	18	16	11	10	10	12	11	12	13	12	12	13	8	
Zn	113	47	34	19	21	22	28	30	43	43	48	27	75	191	64	46	42	51	37	47	55	58
Cu	8	8	5	5	2	6	7	6	7	11	6	20	103	193	8	21	52	14	5	62	164	96
Ni	50	91	57	15	23	31	47	18	80	25	54	125	143	127	114	303	149	74	114	106	120	418
Co	35	35	32	33	33	44	36	29	29	42	35	34	31	38	53	40	48	40	29	35	74	
Cr	109	666	82	31	43	43	55	22	162	45	92	470	1082	484	902	718	459	232	754	619	477	1050
V	260	169	228	247	334	297	353	212	236	255	164	147	151	252	236	185	295	252	162	190	136	
Ce	14	14	12	9	12	10	7	10	12	11	10	17	17	14	11	10	8	9	6	4	12	6
Nd	7	6	4	4	4	4	4	5	4	6	10	12	8	5	4	4	5	4	4	4	6	
Ba	35	54	45	46	23	14	38	36	47	16	30	14	21	36	34	32	23	40	41	36	21	
La	4	4	4	4	7	4	11	4	4	4	4	4	9	9	4	4	7	4	13	4	9	
S	30	3	3	3	3	3	3	3	3	3	3	16	109	279	3	3	3	3	3	3	3	
Hf	1	1	1	4	3	1	3	1	3	3	1	1	5	1	1	3	1	1	1	2	1	
Sc	45	50	54	79	59	57	50	48	43	46	32	30	29	66	84	50	82	89	48	45	72	
As	3	5	6	3	3	7	5	5	4	6	4	3	3	5	7	4	6	4	6	7	7	

Total Fe is expressed as FeO

Table 3. Trace element and REE compositions of the subset of the isotropic gabbro samples analysed by ICP-MS.

Sample	IAT-type isotropic gabbro						Boninitic-type isotropic gabbro							
	KC-30*	KC-35*	KC-39*	KC-41**	KC-46**	Ü-6*	Ü-7*	K-8**	K-27**	K-28*	KC-32**	KC-33**	KC-40*	KC-44**
Ba	19.00	7.1	11.70	4	25	8.70	32	5	< 3	5.6	3	6	3.2	12
Co	31.40	27.4	32.30	26	23	25.10	34	27	25	31.9	37	27	34.7	21
Cs	< 0.1	< .1	< 0.1	< 0.1	< 0.1	< 0.1	< 0.1	< 0.1	< 0.1	< .1	< 0.1	< 0.1	< .1	< 0.1
Ga	13.50	16.9	15.90	14	17	15.30	14	11	9	10.3	10	11	11.2	10
Hf	1.70	1.7	1.00	0.6	1.2	0.80	1.2	0.5	0.2	< .5	0.4	0.5	< .5	0.5
Nb	1.60	2.3	1.50	0.4	1.3	0.70	1.2	0.3	< 0.2	< .5	0.6	0.4	< .5	0.3
Rb	1.20	< .5	0.80	3	2	0.80	2	2	1	< .5	< 1	< 1	< .5	1
Sn	< 1	< 1	< 1	< 1	< 1	< 1	< 1	< 1	< 1	< 1	< 1	< 1	< 1	1
Sr	75.00	129.1	103.60	287	89	130.60	302	143	71	85.1	42	47	176.2	50
Ta	0.10	0.2	0.10	0.02	0.09	< .1	0.07	0.01	< 0.01	< .1	0.05	0.02	< .1	0.02
Th	0.60	0.5	0.30	0.09	0.2	0.20	0.2	0.09	< 0.05	< .1	0.09	0.12	0.1	0.07
U	0.10	0.1	< .1	0.03	0.07	< .1	0.07	0.03	0.01	< .1	0.04	0.04	0.1	0.03
V	164.00	245	301.00	268	188	201.00	267	153	155	156	198	171	198	136
W	< .1	0.2	0.10	< 0.5	< 0.5	< .1	< 0.5	< 0.5	< 0.5	< .1	< 0.5	< 0.5	< .1	< 0.5
Zr	43.20	54.3	30.70	20	36	24.30	35	17	8	4.3	12	15	11.2	14
Y	22.90	27.3	21.30	12.2	23.4	16.50	22.3	8.7	6.4	6.3	9.6	9.7	10.8	9.8
La	2.30	2.6	1.60	0.74	1.86	1.40	1.96	0.64	0.17	< .5	0.5	0.66	< .5	0.52
Ce	5.40	6.1	4.60	2.13	4.98	3.60	5.43	1.81	0.55	0.7	1.16	1.67	1.2	1.43
Pr	0.80	0.94	0.71	0.37	0.82	0.54	0.87	1.86	0.12	0.12	0.18	0.27	0.2	0.25
Nd	5.10	6.3	4.80	2.39	4.96	3.40	5.15	1.86	0.82	0.8	1.21	1.71	1.5	1.68
Sm	1.70	2	1.70	0.92	1.81	1.30	1.88	0.68	0.38	0.3	0.52	0.64	0.7	0.67
Eu	0.62	0.9	0.59	0.383	0.758	0.54	0.815	0.331	0.202	0.21	0.242	0.297	0.29	0.296
Gd	2.39	3.23	2.25	1.43	2.81	1.89	2.78	1.11	0.72	0.66	0.95	1.14	1.26	1.11
Tb	0.51	0.75	0.52	0.29	0.56	0.36	0.54	0.22	0.15	0.17	0.2	0.22	0.26	0.22
Dy	3.23	4.02	3.22	1.94	3.83	2.67	3.65	1.45	1.02	1	1.44	1.56	1.66	1.54
Ho	0.68	0.9	0.68	0.43	0.86	0.56	0.79	0.31	0.23	0.2	0.33	0.35	0.35	0.34
Er	2.28	2.83	2.06	1.36	2.66	1.75	2.4	0.95	0.69	0.7	1.06	1.11	1.07	1.05
Tm	0.33	0.48	0.30	0.207	0.407	0.25	0.355	0.142	0.103	0.11	0.164	0.17	0.18	0.161
Yb	2.33	2.98	2.06	1.31	2.59	1.58	2.21	0.91	0.63	0.59	1.09	1.07	1.11	1.03
Lu	0.31	0.45	0.30	0.191	0.391	0.26	0.326	0.138	0.091	0.09	0.167	0.153	0.21	0.151
Mo	2.50	0.9	1.50	< 2	< 2	1.20	< 2	< 2	< 2	0.6	< 2	< 2	0.2	< 2
Cu	8.30	2.3	3.20	< 10	< 10	4.80	10	20	80	163.5	20	50	2.8	250
Pb	0.10	< .1	< 0.1	< 5	< 5	0.20	< 5	< 5	< 5	0.2	< 5	< 5	0.2	12
Zn	24.00	7	8.00	< 30	< 30	17.00	< 30	< 30	40	157	< 30	< 30	16	150
Ni	47.90	9.4	10.30	40	< 20	13.70	150	110	130	53.3	250	120	30.1	90
As	< .5	< .5	< .5	< 5	< 5	< .5	< 5	< 5	< 5	< .5	< 5	< 5	< .5	< 5
Cd	0.10	< .1	< 0.1	1	1.1	0.10	1.2	1.3	1.3	1.7	1.1	1.1	0.1	1.1
Sb	< .1	< .1	< .1	< 0.2	< 0.2	< .1	< 0.2	< 0.2	< 0.2	< .1	< 0.2	0.4	< .1	< 0.2
Cr	n.a.	n.a.	n.a.	< 20	< 20	n.a.	30	380	900	n.a.	680	440	n.a.	480

na means not analysed

* analysed at Acme Analytical Laboratories Ltd

** analysed at Activation laboratories Ltd

geochemical group (Group I isotropic gabbro and sheeted dike) displays a positive coherent trend, whereas the second geochemical group has lower Zr and TiO₂ contents and is comparable to North Tonga boninites (Figure 8b), although lacking the characteristic Zr enrichment of many

Tertiary boninite suites such as IBM fore-arc boninites and Hunter Ridge boninites (Figure 8b). Differences in terms of V and Ti contents of the both geochemical group can also be observed in Figure 8c. The first geochemical group shows close similarity to IAT or back-arc basin

Table 4. Major and trace element contents of the sheeted dikes from the Kızıldağ (Hatay) ophiolite.

Sample	IAT-type sheeted dikes										Boninitic-type sheeted dikes																			
	AK-15	K-5	K-11	K-13	K-14	K-30	K-29	K-31	KC-31	KC-37	KC-47	KC-51	KC-52	T-11	0-8	0-9	K-4	K-7	K-9	K-12	K-25A	K-29	K-33	KC-22	KC-25	KC-45	KC-49	T-10		
SiO ₂	51.36	49.64	58.89	50.90	53.07	51.28	50.56	54.43	55.21	54.35	52.08	52.14	54.57	53.39	51.34	51.22	49.78	49.89	46.83	50.35	51.92	51.65	52.17	48.94						
TiO ₂	0.71	0.75	0.97	0.73	0.92	0.87	0.82	0.71	1.03	1.04	0.68	0.67	0.69	0.77	1.06	0.58	0.51	0.45	0.56	0.28	0.47	0.61	0.41	0.51	0.40	0.50				
Al ₂ O ₃	15.27	15.15	14.49	15.55	15.76	15.55	15.11	15.00	14.99	15.08	16.24	16.14	15.59	15.51	15.67	14.58	15.57	15.32	15.60	14.14	14.37	14.55	13.29	15.03	13.96	16.44				
FeO*	8.78	10.26	10.80	9.62	8.67	11.25	10.58	7.85	9.73	11.53	9.08	9.02	10.09	6.37	10.85	9.05	7.90	8.47	9.18	9.45	6.35	7.79	8.26	7.86	7.39	7.85	4.29			
MnO	0.15	0.17	0.16	0.16	0.14	0.14	0.17	0.14	0.08	0.09	0.16	0.18	0.12	0.09	0.16	0.20	0.13	0.11	0.23	0.17	0.14	0.12	0.14	0.16	0.08	0.14	0.10			
P ₂ O ₅	0.06	0.06	0.07	0.06	0.06	0.05	0.05	0.07	0.06	0.05	0.06	0.05	0.06	0.08	0.05	0.06	0.04	0.03	0.04	0.04	0.02	0.04	0.05	0.04	0.03	0.02				
LOI	3.80	5.18	1.41	3.17	2.14	2.96	2.92	1.54	1.49	1.28	2.37	6.43	3.18	4.31	4.07	1.25	4.91	0.17	1.56	4.30	2.97	3.52	3.13	4.86						
Cr ₂ O ₃	0.03	0.01	0.00	0.01	0.01	0.00	0.05	0.02	0.01	0.01	0.01	0.01	0.01	0.00	0.05	0.03	0.05	0.10	0.06	0.07	0.03	0.03	0.07	0.01	0.03	0.01				
NiO	0.01	0.01	0.00	0.01	0.00	0.00	0.01	0.01	0.00	0.00	0.01	0.01	0.01	0.00	0.02	0.01	0.01	0.02	0.03	0.02	0.02	0.03	0.01	0.01	0.02	0.01				
Total	99.90	99.88	100.04	99.89	99.67	99.64	99.88	99.94	99.81	99.87	99.99	100.04	100.42	100.32	100.27	100.02	99.46	99.54	100.35	99.80	100.13	100.24	99.65	100.19	99.62	100.04	100.33			
Nb	3	4	4	3	4	4	4	4	6	4	2	2	4	1	4	3	2	2	5	1	1	2	3	4	2	2	1			
Zr	38	37	44	34	40	38	37	35	47	47	34	29	33	40	50	26	24	23	22	20	14	23	31	19	21	19	18			
Y	18	20	26	20	23	22	21	19	25	19	19	21	22	25	18	16	15	16	17	11	15	17	13	18	14	16				
Sr	112	62	382	81	98	85	67	106	99	112	80	83	65	53	150	122	156	69	108	55	55	55	116	68	101	117	37	178		
U	2	2	2	2	2	2	2	2	2	2	2	2	2	2	2	2	2	2	2	2	2	2	3	3	2	2	2			
Rb	6	7	6	7	6	5	4	5	4	5	5	5	4	5	5	6	4	5	4	4	4	4	4	4	4	4	7	10		
Th	3	3	2	3	3	4	2	3	4	4	3	4	4	3	4	3	3	4	3	3	2	2	3	4	3	3	3			
Pb	10	7	12	10	9	11	9	9	11	10	10	12	6	11	9	8	9	12	9	8	12	10	10	10	10	11	4			
Ga	14	13	16	15	14	18	18	13	16	18	14	16	14	17	14	14	12	15	13	11	13	11	12	11	11	11	11			
Zn	42	114	57	65	38	63	50	24	26	31	24	56	40	38	113	101	47	126	58	89	140	63	57	22	30	35				
Cu	9	26	8	106	15	24	41	10	3	8	7	9	13	5	5	84	8	11	77	50	142	41	70	5	6	4	6			
Ni	69	42	13	33	30	26	93	68	28	18	65	53	46	40	17	119	81	91	203	113	112	99	187	78	68	105	64			
Co	38	34	30	39	37	45	35	37	33	41	38	42	36	38	37	38	36	50	41	32	42	43	36	39	39	21				
Cr	200	66	23	464	49	27	576	104	314	30	338	145	568	33	20	282	220	345	352	405	487	448	1495	288	616	359	54			
V	263	295	321	296	367	351	364	269	399	380	271	284	308	286	307	260	261	240	269	229	196	231	225	250	256	230	203			
Ce	9	18	7	15	12	13	18	7	14	13	11	8	11	12	3	8	7	9	11	14	14	12	15	6	6	14				
Nd	6	8	4	7	6	7	9	4	7	6	6	5	6	7	4	6	4	4	6	10	8	5	9	4	4	9				
Ba	37	78	58	50	58	47	11	48	33	17	29	33	28	27	48	71	43	64	55	9	17	40	25	26	49	37	29			
La	7	5	7	7	8	4	6	5	7	8	6	6	7	6	7	5	5	4	10	4	6	4	4	4	4	4				
S	55	3	3	3	3	3	3	22	3	3	3	3	3	3	3	55	3	14	3	9	375	30	72	3	3	3	7			
Hf	1	2	5	4	5	2	4	4	5	1	3	1	3	1	3	6	1	1	1	1	1	1	1	1	1	1				
Sc	41	54	40	65	55	55	44	70	52	47	60	56	48	41	69	35	41	36	43	55	46	44	44	44	44	34	34			
As	3	3	3	3	4	3	3	3	3	4	3	3	4	4	3	3	4	3	4	3	3	4	3	3	3	3	3			

Total Fe is expressed as FeO*.

Table 5. Trace element and REE compositions of the subset of the sheeted dike samples analysed by ICP-MS.

Sample	IAT - type sheeted dike						Boninitic-type sheeted dike								
	K-5**	K-13**	K-14*	KC-29*	KC-37*	KC-51*	U-8**	K-4**	K-12**	K-25A**	K-29**	K-33*	KC-22**	KC-25*	KC-49**
Ba	34	12	20.60	3	4.80	12.6	< 3	25	11	9	4	31.8	< 3	5.70	4
Co	24	24	32.00	37.9	33.00	36.1	30	29	35	34	25	36.8	29	37.90	27
Cs	0.1	< 0.1	< 0.1	< .1	< 0.1	< .1	< 0.1	< 0.1	< 0.1	< 0.1	< 0.1	< .1	< 0.1	< 0.1	< 0.1
Ga	12	14	15.30	20.2	16.70	15.4	13	12	12	13	10	11.4	12	9.80	11
Hf	1.1	1	1.20	1.4	1.40	1.1	1.1	0.8	0.6	0.6	0.3	0.6	0.8	0.50	0.5
Nb	0.9	0.6	1.00	2.4	3.00	1	1.1	0.7	0.9	0.4	< 0.2	0.6	0.9	1.40	0.6
Rb	4	3	1.90	< .5	1.10	< .5	1	2	< 1	< 1	< 1	< .5	< 1	0.70	2
Sn	< 1	< 1	< 1	< 1	< 1	< 1	< 1	< 1	< 1	< 1	< 1	< 1	< 1	< 1	< 1
Sr	58	76	107.00	82.8	108.70	88	50	111	111	54	54	127.9	71	118.10	35
Ta	0.05	0.03	< .1	0.1	0.20	< .1	0.11	0.05	0.06	0.05	< 0.01	< .1	0.05	< .1	0.03
Th	0.18	0.16	0.50	0.5	1.10	< .1	0.19	0.16	0.17	0.06	< 0.05	< .1	0.18	0.30	0.14
U	0.07	0.05	0.20	< .1	0.40	< .1	0.06	0.06	0.06	0.02	0.02	< .1	0.06	< .1	0.03
V	243	247	312.00	325	339.00	250	286	209	218	228	200	201	198	217.00	185
W	< 0.5	< 0.5	0.20	0.6	0.30	0.1	8.7	< 0.5	< 0.5	< 0.5	< 0.5	< .1	< 0.5	0.10	< 0.5
Zr	32	30	35.80	31.8	44.50	27.4	33	23	21	17	10	15.9	25	13.20	17
Y	18.7	17.2	23.70	23.9	26.80	19	21.1	15.2	13.8	15.4	8.4	13.9	15.1	10.70	11
La	1.3	1.34	1.70	2.6	3.90	1.2	1.86	1.06	1.02	0.75	0.31	0.8	1.41	1.00	0.59
Ce	3.72	3.75	4.70	5.4	7.70	3.6	5.28	2.84	2.42	2.18	0.93	2.1	3.56	2.00	1.5
Pr	0.65	0.65	0.82	0.79	1.02	0.57	0.84	0.49	0.38	0.41	0.18	0.36	0.57	0.27	0.26
Nd	3.94	3.99	4.70	4.7	5.90	3.7	4.96	3.08	2.27	2.73	1.17	2.4	3.43	1.70	1.64
Sm	1.41	1.4	1.80	1.6	2.10	1.4	1.8	1.15	0.82	1.11	0.49	0.9	1.28	0.70	0.64
Eu	0.583	0.585	0.76	0.76	0.74	0.61	0.799	0.483	0.399	0.521	0.252	0.49	0.567	0.23	0.292
Gd	2.3	2.16	2.66	2.67	2.99	2.22	2.65	1.81	1.47	1.84	0.9	1.72	1.91	1.00	1.17
Tb	0.45	0.42	0.55	0.6	0.63	0.41	0.52	0.36	0.29	0.37	0.19	0.34	0.36	0.26	0.24
Dy	3.02	2.82	3.65	3.51	4.12	2.72	3.43	2.49	2.01	2.54	1.35	2.18	2.46	1.58	1.64
Ho	0.66	0.62	0.75	0.83	0.88	0.61	0.75	0.55	0.46	0.56	0.3	0.5	0.54	0.36	0.37
Er	2.05	1.92	2.58	2.37	2.55	1.87	2.28	1.72	1.45	1.76	0.95	1.39	1.66	1.22	1.18
Tm	0.315	0.291	0.34	0.38	0.38	0.3	0.347	0.262	0.229	0.266	0.149	0.23	0.249	0.17	0.184
Yb	2	1.84	2.40	2.55	2.88	2.02	2.21	1.66	1.45	1.67	0.94	1.47	1.58	1.49	1.2
Lu	0.291	0.265	0.34	0.39	0.39	0.25	0.332	0.233	0.208	0.24	0.129	0.2	0.23	0.18	0.182
Mo	< 2	< 2	0.90	0.5	1.20	0.2	< 2	< 2	< 2	< 2	< 2	0.7	< 2	0.60	< 2
Cu	30	100	13.40	65.7	2.10	3.1	10	90	100	40	100	30.2	70	2.50	< 10
Pb	< 5	< 5	0.10	0.1	0.10	0.3	< 5	< 5	< 5	< 5	< 5	1.8	< 5	0.20	< 5
Zn	60	40	49.00	38	15.00	12	30	60	100	60	50	126	30	34.00	< 30
Ni	30	30	9.70	62.4	16.30	16.1	40	100	180	100	100	38.2	130	52.40	90
As	< 5	< 5	< .5	< .5	< .5	< .5	< 5	< 5	28	< 5	< 5	< .5	< 5	< .5	< 5
Cd	1.2	0.8	0.40	0.1	0.10	0.1	1.3	1.3	0.8	1.3	1.4	0.5	1.4	0.10	1.4
Sb	< 0.2	< 0.2	< .1	< .1	< .1	< .1	< 0.2	0.5	1.2	< 0.2	< 0.2	1.7	< 0.2	< .1	< 0.2
Bi	< 0.1	< 0.1	< .1	< .1	< .1	< .1	< 0.1	< 0.1	0.2	< 0.1	< 0.1	< .1	< 0.1	< .1	< 0.1
Ag	< 0.5	< 0.5	< .1	< .1	< .1	< .1	< 0.5	< 0.5	< 0.5	< 0.5	< 0.5	< .1	< 0.5	< .1	< 0.5
Cr	30	70	n.a.	n.a.	n.a.	n.a.	20	230	510	320	360	n.a.	340	n.a.	340

na means not analysed

* analysed at Acme Analytical Laboratories Ltd

** analysed at Activation laboratories Ltd

basalt (BABB), whereas the second geochemical group has very low Ti contents and overlaps with the boninite field (Figure 8c).

The chondrite normalized REE and N-MORB normalized spider diagrams for the first geochemical group (Group I isotropic gabbros and sheeted dikes) are presented in Figure 9. The REE concentrations vary from 3.12 to 20.05 X chondritic for isotropic gabbros and from 5.06 to 16.94 X chondritic for sheeted dikes. They

have slightly LREE-depleted patterns ($\text{La}_{\text{N}}/\text{Yb}_{\text{N}} = 0.41$ to 0.71 for isotropic gabbros and $\text{La}_{\text{N}}/\text{Yb}_{\text{N}} = 0.43$ to 0.97) for sheeted dikes (Figure 9a, c). The spider diagrams of the first geochemical group exhibits such features as (a) enrichment in LIL (i.e. Cs, Rb, Ba, Th, K) elements, (b) positive Sr anomaly, (c) negative Nb and Ta anomalies and (d) flat and slightly depleted patterns of HFS elements relative to N-MORB (Figure 9b, d). Within the LIL element group Th is a relatively stable and reliable indicator, and

Table 6. Major and trace element contents of the sakkalites from the Kızıldağ (Hatay) ophiolite.

Sample	Hyaloclastites							Pillows										
	SKL 1	SKL 4	SKL 6	SKL 9	SKL 11	SKL 12	SKL 13	SKL 15	SKL 17	SKL 2	SKL 3	SKL 5	SKL 8	SKL 10	SKL 14	SKL 16	SKL 18	
SiO ₂	49.51	49.96	48.76	48.71	53.11	49.33	47.53	49.67	48.51	50.78	51.10	51.26	51.53	50.35	51.38	51.09	50.47	51.46
TiO ₂	0.33	0.34	0.34	0.34	0.29	0.32	0.31	0.32	0.33	0.36	0.34	0.35	0.37	0.34	0.35	0.35	0.34	0.34
Al ₂ O ₃	13.46	13.29	13.39	13.35	12.78	13.01	12.49	13.06	13.00	14.15	14.02	14.05	14.28	13.85	14.10	14.26	13.98	14.05
FeO*	8.01	8.02	7.75	8.60	7.71	7.76	8.10	7.72	8.36	8.53	8.43	8.19	8.64	8.59	8.58	8.58	8.18	8.18
MnO	0.18	0.18	0.17	0.17	0.16	0.15	0.17	0.15	0.17	0.16	0.19	0.16	0.17	0.19	0.15	0.19	0.16	0.16
MgO	8.96	9.00	8.70	8.48	9.74	8.63	8.85	8.69	8.96	9.25	9.02	9.53	8.92	9.17	9.52	9.83	9.59	8.76
CaO	7.75	7.69	7.72	7.93	10.07	8.12	13.67	8.66	6.90	10.71	10.72	10.89	11.37	10.16	10.84	11.15	11.24	11.24
Na ₂ O	1.10	1.57	1.53	1.41	1.09	0.75	0.72	0.76	0.55	1.57	1.17	1.24	1.16	1.20	1.43	0.92	1.00	1.00
K ₂ O	0.32	0.24	0.29	0.26	0.55	0.30	0.25	0.25	0.27	0.24	0.18	0.19	0.15	0.18	0.26	0.21	0.30	0.14
P ₂ O ₅	0.02	0.02	0.02	0.02	0.02	0.02	0.02	0.02	0.02	0.02	0.02	0.02	0.02	0.02	0.02	0.02	0.03	0.03
LOI	10.13	9.25	10.81	11.19	3.26	11.35	8.19	9.70	13.38	3.95	4.39	3.67	3.80	4.72	3.79	3.56	4.28	4.26
Cr ₂ O ₃	0.08	0.08	0.08	0.08	0.13	0.09	0.08	0.09	0.10	0.09	0.10	0.09	0.09	0.08	0.10	0.08	0.09	0.10
NiO	0.04	0.03	0.04	0.03	0.04	0.03	0.03	0.03	0.03	0.03	0.03	0.03	0.03	0.03	0.03	0.03	0.03	0.03
Toplam	99.88	99.66	99.87	99.71	99.84	99.81	100.12	99.51	99.95	99.66	99.81	99.85	99.83	99.69	99.97	99.93	99.94	99.76
Nb	4	4	4	4	4	4	2	5	4	2	5	2	3	2	3	3	3	4
Zr	18	18	18	18	15	18	19	18	19	19	18	19	20	19	17	19	17	20
Y	12	12	13	12	12	13	12	23	13	13	13	13	13	13	17	17	13	14
Sr	87	78	81	78	34	82	85	67	66	75	57	51	43	62	72	40	70	42
U	2	2	2	2	3	2	3	2	2	2	2	2	2	2	2	3	2	2
Rb	9	8	8	8	10	10	10	10	10	8	7	7	7	7	7	8	7	7
Th	3	4	2	3	3	3	4	3	3	3	4	4	3	3	3	4	2	2
Pb	11	12	13	10	12	12	9	12	10	12	11	12	11	11	12	13	12	10
Ga	12	12	11	11	10	11	11	11	11	11	11	12	13	11	12	13	12	12
Zn	62	60	81	62	63	58	53	58	58	62	64	65	60	65	64	66	66	61
Cu	87	90	90	33	88	97	93	88	92	101	97	106	91	98	94	103	107	107
Ni	224	207	235	210	232	202	166	184	230	176	202	215	181	203	215	215	200	175
Co	40	42	43	43	44	43	44	46	47	45	46	45	39	44	45	47	45	42
Cr	638	492	536	472	890	539	497	516	510	460	609	596	612	490	567	599	532	671
V	213	233	227	205	172	207	204	219	241	223	240	224	248	217	248	232	230	230
Ce	9	6	9	10	15	15	5	11	4	6	4	4	4	6	7	7	4	8
Nd	5	4	4	6	10	11	4	6	4	4	4	4	4	4	6	4	5	5
Ba	62	66	75	48	61	39	57	76	43	41	43	39	51	57	37	49	45	45
La	7	4	4	6	5	4	4	6	4	7	7	4	4	6	4	7	5	5
S	75	8	27	13	3	20	124	3	3	51	114	127	209	96	61	3	76	223
Hf	1	3	1	1	1	1	2	2	3	1	1	1	1	4	2	2	1	1
Sc	61	53	54	52	60	56	25	53	64	39	44	37	43	36	43	38	39	45
As	3	3	3	5	4	4	4	3	3	3	3	3	3	3	3	3	3	3

Total Fe is expressed as FeO

Table 7. Trace element and REE compositions of the subset of the sakalavite samples analysed by ICP-MS.

Sample	Hyaloclastites		Pillows			
	SKL-1*	SKL-6*	SKL-3*	SKL-8*	SKL-10*	SKL-16*
Ba	20.60	26.4	21.9	19.1	28.30	21.30
Co	35.20	39.5	41.8	40.5	39.20	39.60
Cs	0.10	0.2	0.2	0.1	0.20	0.10
Ga	10.10	11.4	12.4	11.9	10.80	11.50
Hf	0.60	0.6	0.5	0.6	< 0.5	< 0.5
Nb	0.90	1.2	1	1.1	0.80	0.90
Rb	5.80	4.5	3.6	3.7	4.30	4.00
Sn	< 1	< 1	1	2	< 1	< 1
Sr	86.40	86.5	53.9	67.9	76.70	76.80
Ta	< .1	< .1	< .1	< .1	< .1	< .1
Th	< .1	< .1	0.1	0.1	0.10	< .1
U	< .1	< .1	< .1	< .1	< .1	< .1
V	177	212	242	226	230	224
W	< .1	0.2	0.2	0.2	0.10	0.10
Zr	10.40	13	10.9	11.4	10.20	9.90
Y	9.40	10.9	11.3	11.7	12.40	12.00
La	0.60	0.7	0.7	0.7	0.70	0.60
Ce	1.10	1.3	1.2	1.3	1.40	1.20
Pr	0.18	0.24	0.22	0.24	0.18	0.20
Nd	1.30	1.1	1.1	0.9	0.80	1.10
Sm	0.50	0.6	0.7	0.6	0.60	0.60
Eu	0.25	0.26	0.24	0.26	0.28	0.28
Gd	0.90	1.06	0.96	1.13	1.02	1.13
Tb	0.18	0.23	0.28	0.26	0.27	0.28
Dy	1.50	1.43	1.51	1.59	1.82	1.70
Ho	0.32	0.37	0.38	0.37	0.40	0.40
Er	0.94	1.04	1.1	1.24	1.30	1.20
Tm	0.14	0.18	0.21	0.2	0.19	0.20
Yb	1.08	1.23	1.3	1.46	1.46	1.30
Lu	0.15	0.19	0.23	0.19	0.22	0.19
Mo	0.50	1.3	2.3	0.8	0.80	0.60
Cu	55.70	62.3	40.5	45.1	61.50	65.30
Pb	0.40	6.2	0.3	0.4	0.80	0.50
Zn	35.00	90	18	18	24.00	29.00
Ni	180.10	170.4	134.6	144.7	141.60	149.30
As	< .5	0.8	< .5	< .5	< .5	< .5
Cd	0.10	0.2	< .1	0.1	0.10	0.10
Sb	< .1	2.2	< .1	< .1	< .1	0.10

* analysed at Acme Analytical Laboratories Ltd

its enrichment relative to other incompatible elements is taken to record the subduction zone component (Wood *et al.* 1979; Pearce 1983). Likewise, the negative Nb anomaly may indicate a subduction-related tectonic

setting for the first geochemical group (Arculus & Powell 1986; Yogodzinski *et al.* 1993; Wallin & Metcalf 1998). The second geochemical group (Group II isotropic gabbros, sheeted dikes and sakalavites), however, differs

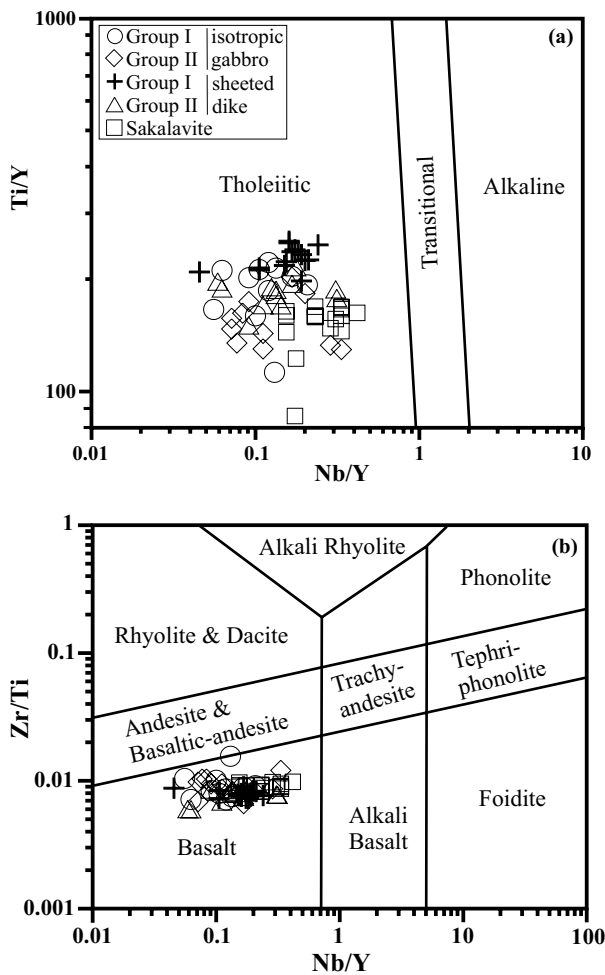


Figure 6. (a) Ti/Y vs Nb/Y (after Pearce 1982) and (b) Zr/Ti vs Nb/Y (after Pearce 1996) diagrams for the crustal rocks of the Kizildağ (Hatay) ophiolite.

from the first geochemical group in both REE profiles and multi-element patterns (Figure 10). The REE concentrations vary from 0.71 to 8.27 X chondritic for isotropic gabbros, from 1.31 to 10.63 X chondritic for sheeted dikes and from 1.71 to 9.06 X chondritic for sakalavites. They exhibit spoon-shaped REE patterns typical of boninites (Figure 10), with $\text{La}_{\text{N}}/\text{Sm}_{\text{N}}$ and $\text{Sm}_{\text{N}}/\text{Yb}_{\text{N}}$ ratios ranging from 0.29 to 0.92 and from 0.46 to 0.90, respectively. The N-MORB normalized multi-element diagrams of the second geochemical group indicate that they are generally depleted in HFS and enriched in some of LIL elements (Cs, Rb, Ba, K) (Figure 10b, d, f). The REE and multi-element patterns indicate that the second geochemical group (Group II isotropic gabbros, sheeted dikes and sakalavites) are

compositionally very similar to boninitic magmas found in the fore-arc regions of oceanic island arcs (Crawford *et al.* 1989; Falloon & Crawford 1991).

The Th/Yb versus Ta/Yb plot is included in the MORB-OIB array and thus discriminates between depleted mantle (MORB) and enriched mantle (intraplate) sources (Pearce 1982) (Figure 11). For subduction-related magmatic rocks, addition of a subduction chemical component by slab-derived fluids/melts results in an increase in Th/Yb in the mantle source as shown by the arrow in Figure 11. The data from the selected samples of the isotropic gabbros and sheeted dikes is consistent with derivation for a MORB-type depleted mantle source enriched by subduction zone fluids (Figure 11).

Petrogenesis

The first geochemical group (Group I isotropic gabbros, sheeted dikes) in the Kizildağ (Hatay) ophiolite displays strong depletion of Nb (Ta) and enrichment of LIL elements. These rocks also exhibit parallel to slightly depleted HFS element patterns compared to N-MORB. Their negative Nb (Ta) and positive Th anomalies clearly indicate a suprasubduction zone tectonic environment. Similar flat to slightly LREE-depleted patterns have been found in island arc tholeiitic series, namely in Papua New Guinea, the Solomon Islands, Macquarie Island (Jakes & Gill 1970), and suprasubduction zone-type ophiolites of the eastern Mediterranean region (Alabaster *et al.* 1982; Meffre *et al.* 1996; Parlak 1996; Yalınız *et al.* 1996; Parlak *et al.* 2000; Al-Riyami *et al.* 2002; Beccaluva *et al.* 2004, 2005; Pe-Piper *et al.* 2004; Saccani & Photiades 2005; Rızaoglu *et al.* 2006; Bağcı & Parlak 2007).

Experimental studies on boninite petrogenesis indicate that this magma type is generated from either a clinopyroxene-poor lherzolite or, more commonly, a harzburgite source at low pressures, probably less than 10 kbar for realistic H_2O contents in this magma (< 5 %) (Green 1976; Tatsumi 1982; Cawthorn & Davies 1983; Jenner 1983). A depleted or refractory magma source for the boninites is indicated by their low TiO_2 contents, which result in high CaO/TiO_2 and $\text{Al}_2\text{O}_3/\text{TiO}_2$ values and low Ti/V and Ti/Sc values (Crawford *et al.* 1989 and references therein). Based on the definition of Crawford *et al.* (1989), boninites are divided into two classes, low-Ca and high-Ca suites. The second geochemical group (Group II isotropic gabbros, sheeted dikes and

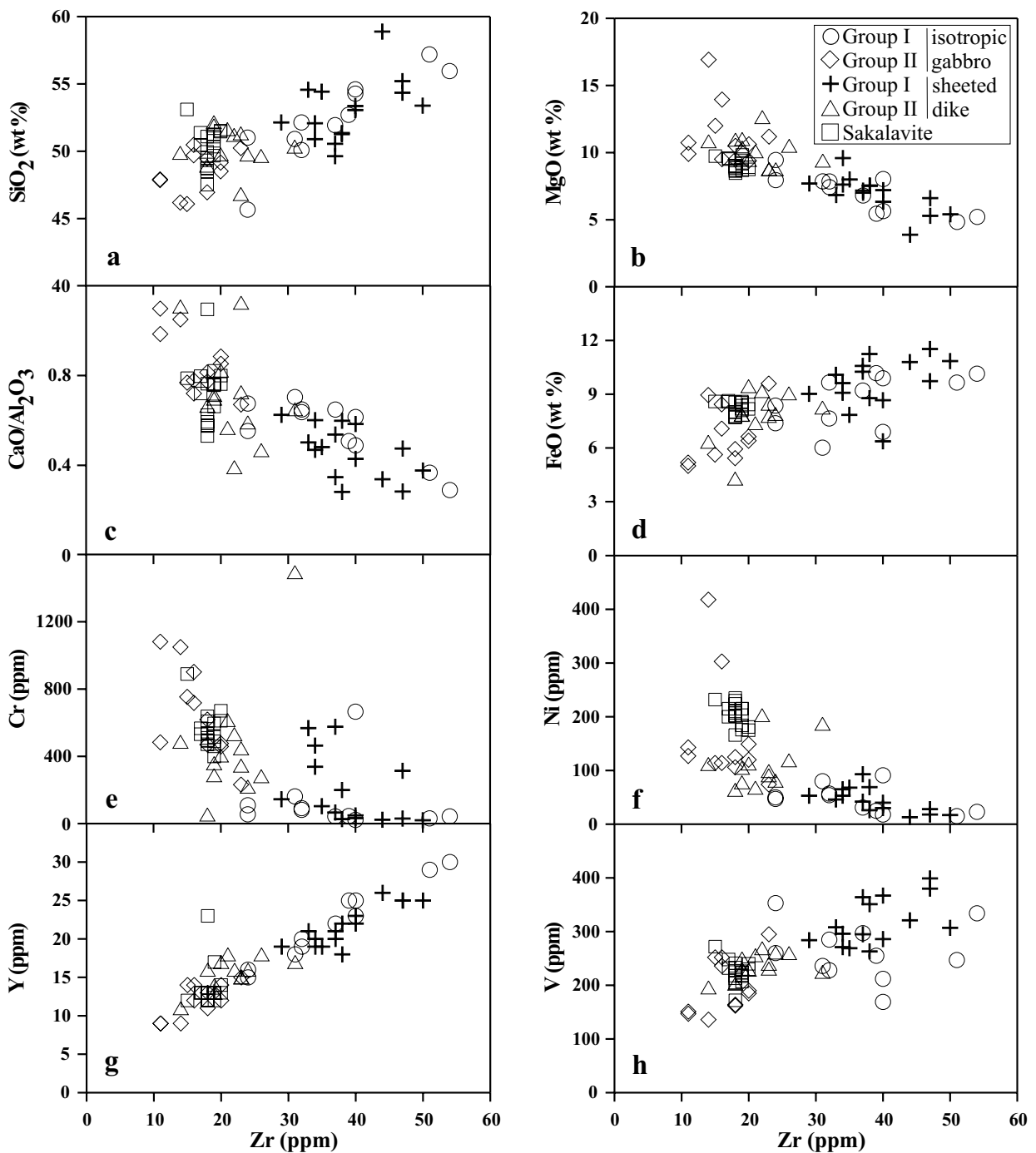


Figure 7. Variations of selected major and trace element contents of the crustal rocks of the Kızıldağ (Hatay) ophiolite.

sakalavites) are basaltic in composition and have silica contents between 46.09 and 52.17 wt%. Their $\text{CaO}/\text{Al}_2\text{O}_3$ ratios and FeO contents vary from 0.39 to 1.12 and from 4.29 to 9.6 wt%, respectively. The total alkali contents are between 0.41 and 4.19 wt%.

The major element geochemistry of the second geochemical group (Group II isotropic gabbros, sheeted dikes and sakalavites) from the Kızıldağ (Hatay) ophiolite are very similar to high-Ca boninites and very comparable with the Upper Pillow Lava unit of the Troodos ophiolite

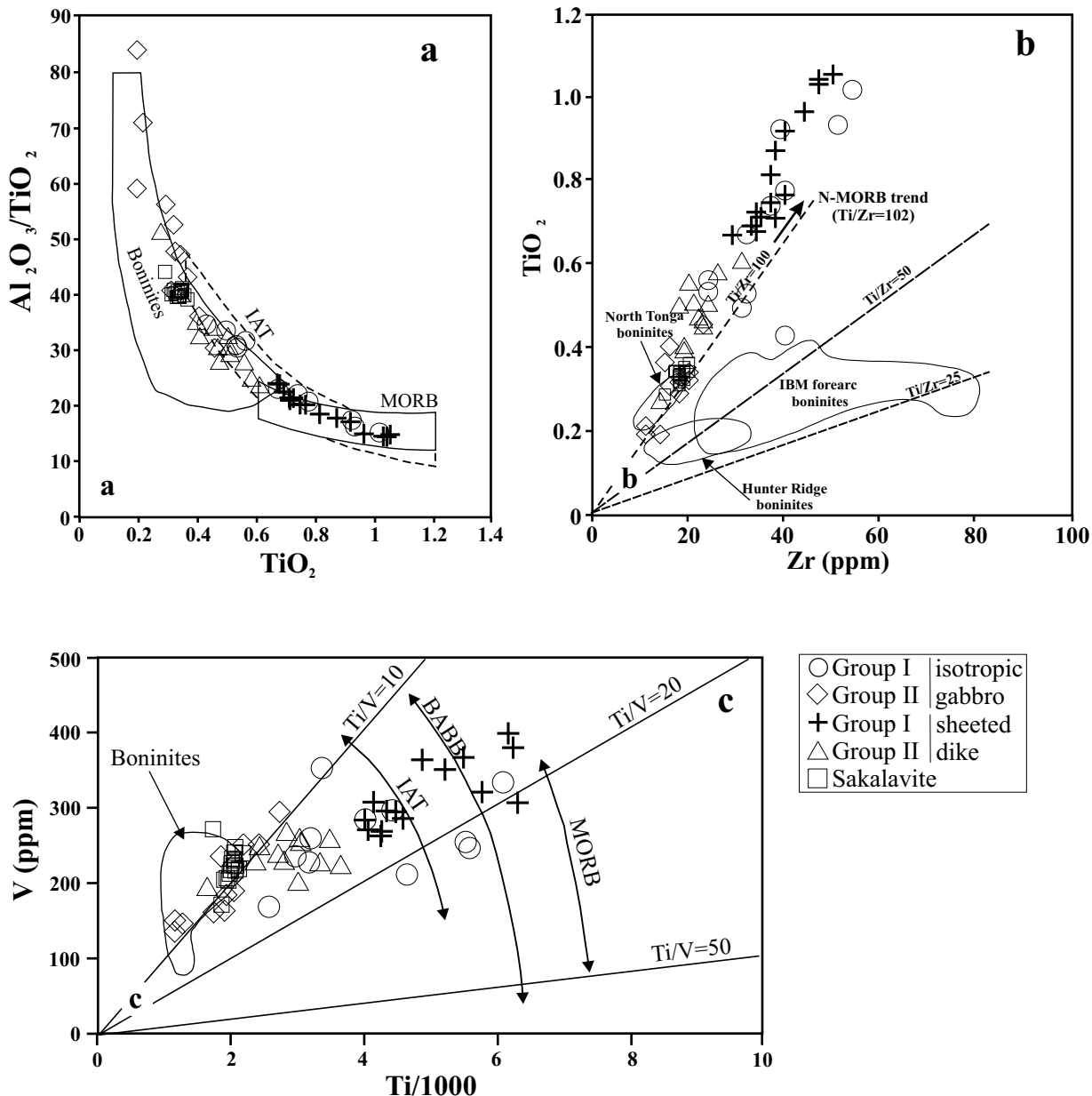


Figure 8. (a) $\text{Al}_2\text{O}_3/\text{TiO}_2$ vs TiO_2 , (b) Zr vs TiO_2 , and (c) V vs Ti variations for the crustal rocks of the Kizildag (Hatay) ophiolite. Data for Boninites, MORB and IAT from Hickey & Frey (1982); Crawford (1989). Ranges of Ti/V ratios for IAT, BAB and MORB from Shervais (1982). North Tonga from Falloon & Crawford (1991), IBM fore-arc from Arculus *et al.* (1992) and Wood *et al.* (1982), Hunter Ridge from Meffre *et al.* (1996).

(Crawford *et al.* 1989), as well as typical boninitic rocks from various ophiolitic complexes (Beccaluva *et al.* 1984, 2005; Malpas & Langdon 1984; Beccaluva & Serri 1988; Smellie *et al.* 1995; Meffre *et al.* 1996; Bedard *et al.* 1998; Bedard 1999; Pearce 2003; Pe-Piper *et al.* 2004; Saccani & Photiades 2004, 2005; Parlak 2006; Bağcı & Parlak 2007).

A Cr versus Y diagram for estimating the composition of mantle sources, and the degree of partial melting that generates different magma types (Pearce 1983) also plots the trend of N-MORB for comparison. On this diagram the studied rocks were clearly derived from an already-depleted lherzolitic to harzburgitic mantle composition (Figure 12). The first and second magma

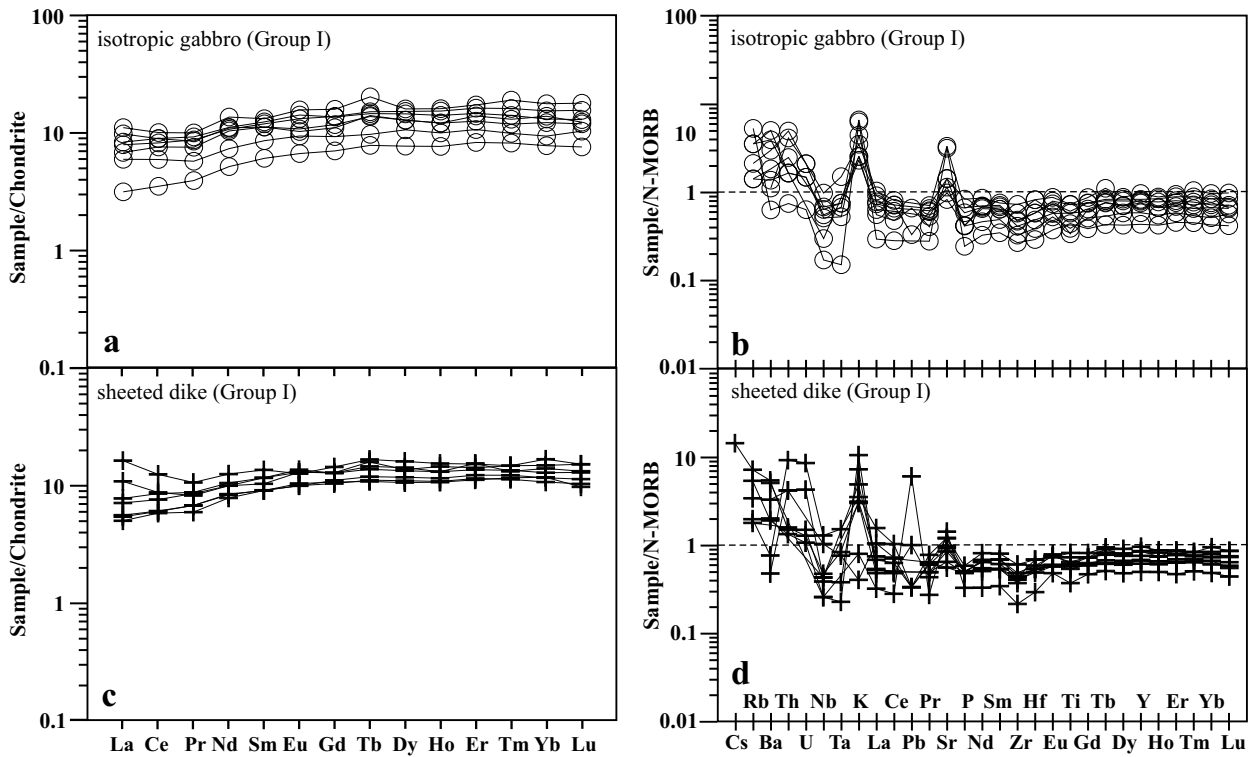


Figure 9. Chondrite-normalized REE (a, c) and N-MORB normalized spider diagrams (b, d) for the isotropic gabbroic and sheeted dike rocks from the Kızıldağ (Hatay) ophiolite (normalizing values are from Sun & McDonough 1989).

series (IAT and boninite) from the Kızıldağ (Hatay) ophiolite are plotted in Figure 12. The first geochemical group (Group I isotropic gabbros and sheeted dikes) have relatively higher REE contents, thus representing magmas generated from the less depleted mantle sources. These rocks may have been derived from approximately 12–17% partial melting from a mantle source that experienced previous MORB melt extraction at about 20% (M2) (Figure 12). In contrast, the second geochemical group (Group II isotropic gabbros, sheeted dikes and sakalavites) have progressively lower REE contents, which may result from the higher degrees of partial melting of same refractory mantle sources. Thus, this geochemical group may have been derived from approximately 17–25% partial melting of a M2 source (Figure 12).

Discussion and Conclusion

The south Neotethyan ophiolites formed around 90 Ma (Mukasa & Ludden 1987) in a suprasubduction zone

setting (Lytwyn & Casey 1993; Dilek & Thy 1998; Robertson 1986a, b, 2002; Parlak *et al.* 2004; Bağci *et al.* 2005; Parlak 2006; Rızaoglu *et al.* 2006). The southern branch of Neotethys comprises well-documented ophiolites such as the Tekirova (Antalya), Kızıldağ (Hatay), Göksun (Kahramanmaraş), İspendere (Malatya), Kömürhan-Guleman (Elazığ) in Turkey (Parlak *et al.* 2004; Bağci *et al.* 2005; Rızaoglu *et al.* 2006), the Troodos in Cyprus (Robertson 1998, 2000; Dilek & Flower 2003) and Baer-Bassit in Syria (Al-Riyami *et al.* 2002).

Modern boninites are mainly restricted to fore-arc environments (Cameron *et al.* 1979; Meijer *et al.* 1980; Hawkins *et al.* 1984; Murton 1989; Stern & Bloomer 1992). Rare examples of boninites have also been reported from the Lau back-arc basin (Falloon *et al.* 1992). Fore-arc regions in modern environments are characterized by significant extensional tectonism due to true seafloor-spreading (Meijer 1980; Bloomer & Hawkins 1983; Stern & Bloomer 1992; Taylor & Nesbitt 1994; Wessel *et al.* 1994). Boninitic lavas and intrusions

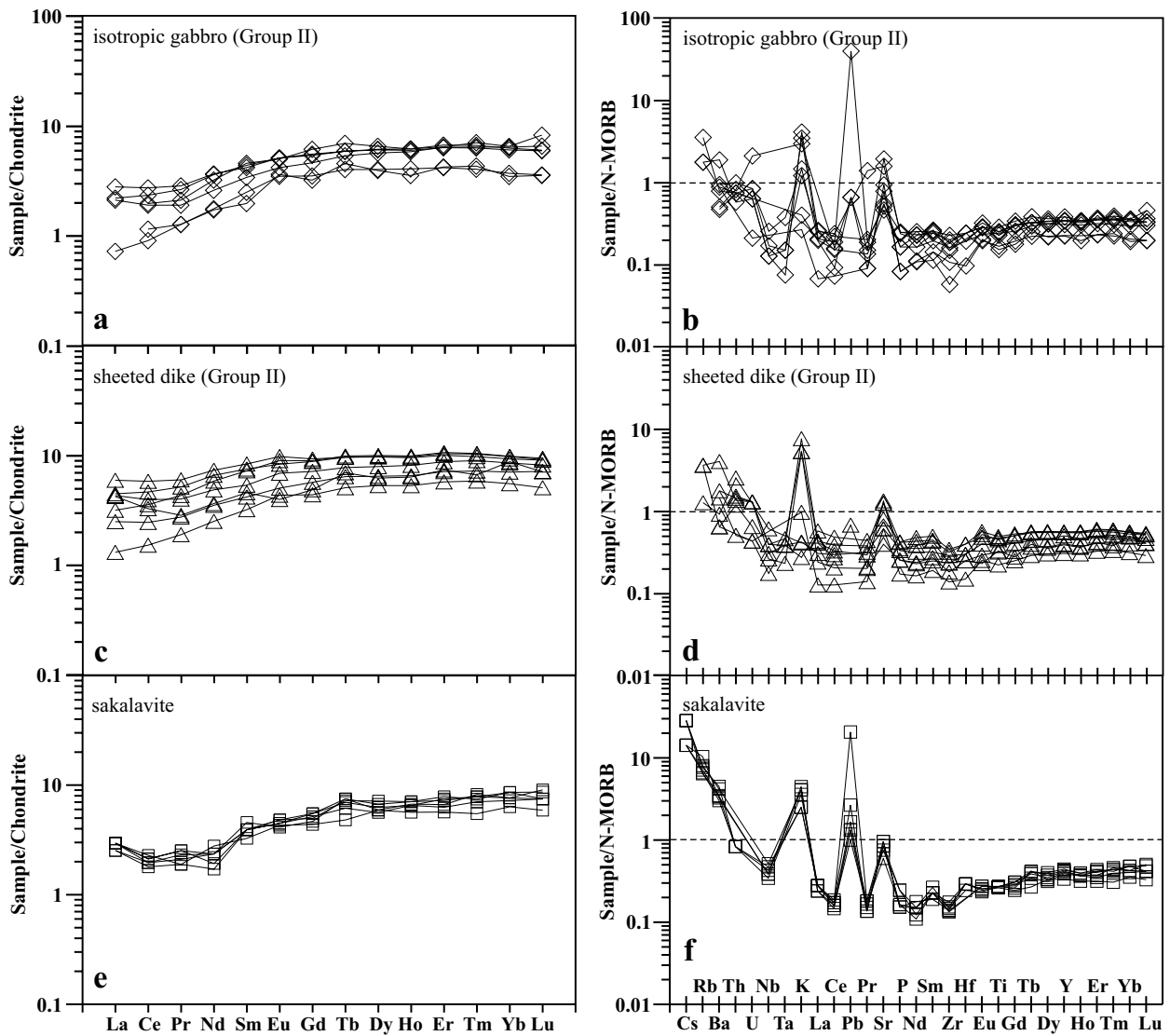


Figure 10. Chondrite-normalized REE (a, c, e) and N-MORB normalized spider diagrams (b, d, f) for the isotropic gabbros, sheeted dikes and sakalavites from the Kızıldağ (Hatay) ophiolite (normalizing values are from Sun & McDonough 1989).

have been reported from many ophiolite complexes (Bedard *et al.* 1998 and references therein).

Due to opening of the South Atlantic ocean at the end of the Early Cretaceous the southern branch of the Neotethyan ocean between the Eurasian and African plates started to close (Livermore & Smith 1984; Savostin *et al.* 1986; Dilek *et al.* 1990, 1999). Northward subduction occurred in the southern Neotethyan oceanic basin as a result of this convergent regime. Subduction-related ophiolites in the southern Neotethyan oceanic basin formed above this north-

dipping subduction zone (Dilek *et al.* 1999; Beyarslan & Bingöl 2000; Al-Riyami *et al.* 2002; Parlak *et al.* 2004; Bağcı *et al.* 2005, 2006; Rızaoğlu *et al.* 2006). These are, from west to east, Tekirova (Antalya), Troodos (Cyprus), Kızıldağ (Hatay), Baer-Bassit (Syria), Göksun (Kahramanmaraş), İspendere (Malatya), Kömürhan and Guleman (Elazığ).

The Kızıldağ ophiolite displays structural evidence for seafloor-spreading tectonics and associated structural, magmatic and hydrothermal processes (Erendil 1984; Robertson 1986a, b; Tekeli & Erendil 1986; Pişkin *et al.*

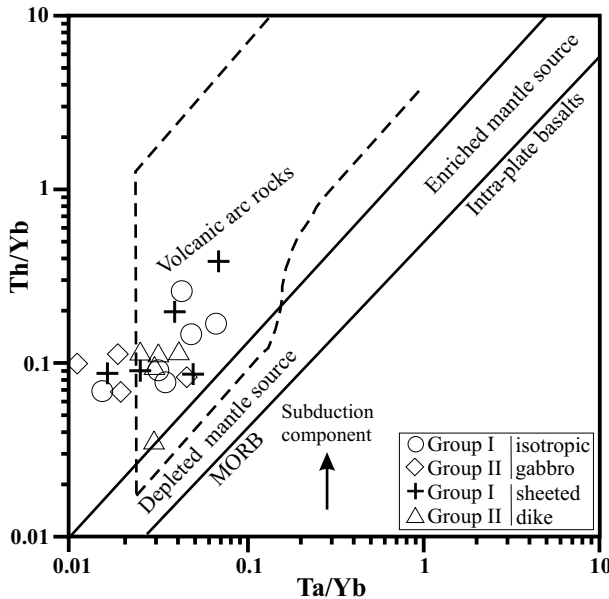


Figure 11. Ta/Yb vs Th/Yb diagram (after Pearce 1982) for the crustal rocks of the Kızıldağ (Hatay) ophiolite.

1990; Dilek *et al.* 1991; Dilek & Delaloye 1992; Dilek & Eddy 1992; Lytwyn & Casey 1993; Dilek & Thy 1998). Bağci *et al.* (2005) presented detailed mineral chemistry data on the cumulate rocks of the Kızıldağ (Hatay) ophiolite and suggested its formation in a suprasubduction zone setting. New geochemical data presented in this paper from the isotropic gabbros, sheeted dikes and the volcanics (sakalavites) of the Kızıldağ (Hatay) ophiolite suggest that two main types of basic magmas formed the oceanic crust in the Late Cretaceous. These are (i) IAT series which can be referred to the Group I isotropic gabbros and sheeted dikes; (ii) Low-Ti boninitic series characterized by the Group II isotropic gabbros, sheeted dikes and sakalavites. The spatial and temporal relations of the boninitic magmatism relative to associated arc tholeiites in the Kızıldağ (Hatay) ophiolite is well constrained in this study. Tables 8 to 10 summarize the localities, geochemical affinities and spatial and temporal relations of the isotropic gabbros, sheeted dykes and sakalavites from the Kızıldağ ophiolite. In the Çevlik (Güvercinkaya burnu) region, the IAT-type sheeted dykes (K-11) were cut by plagiogranite which was in turn intruded by the boninitic-type sheeted dykes (K-9 and K-12) (Figure 13a, b). In the Karaçay valley, the boninitic-type dyke (KC-22) intruded the cumulate gabbro (Figure 13c) and in the same valley the boninitic

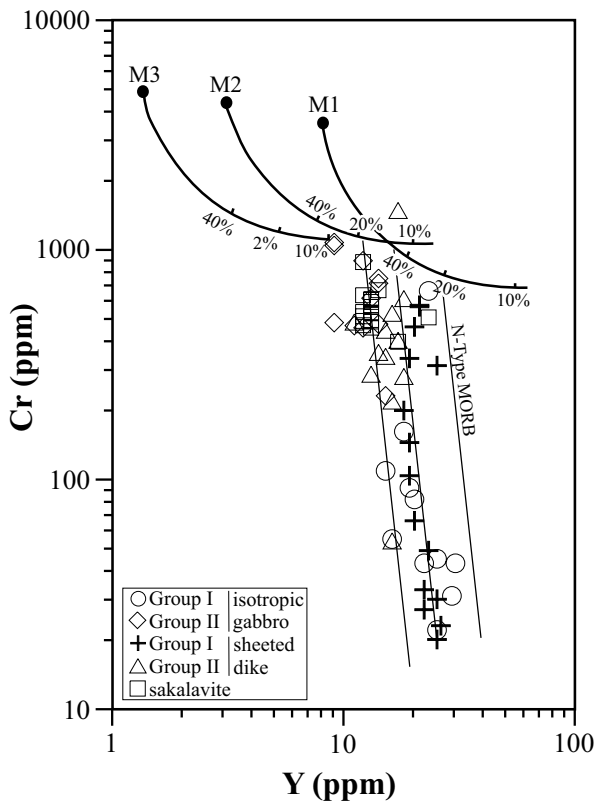


Figure 12. Cr vs Y diagram for the isotropic gabbros, sheeted dikes and sakalavites from the Kızıldağ (Hatay) ophiolite. Mantle source compositions and melting paths for incremental batch melting are from Murton (1989). M1—calculated mid-ocean ridge basalt (MORB) source; M2—residue after 20% MORB extraction; M3—residue after 12% melt extraction from M2.

type isotropic gabbro (KC-28) was cut by the IAT-type dyke (KC-29) (Figure 13d). Apart from these, there is plenty of field and geochemical evidence from different localities suggesting that IAT- and boninitic-type magmatism were contemporaneously active in forming the different parts of the crustal units of the Kızıldağ ophiolite in a fore-arc tectonic setting in the southern Neotethys ocean during the late Cretaceous (Tables 8 to 10).

In the Mariana fore-arc region, boninites overlie arc tholeiites (Wood *et al.* 1981; Hickey & Frey 1982). In Guam, arc tholeiites cap boninites (Reagan & Meijer 1984). In the Cape Vogel area, two boninite series of Paleocene age overlie island arc tholeiites (Jenner 1981; Walker & Cameron 1983). In the Troodos ophiolite, boninite magmatism (Upper Pillow Lava) occurred both contemporaneously and after emplacement of island arc

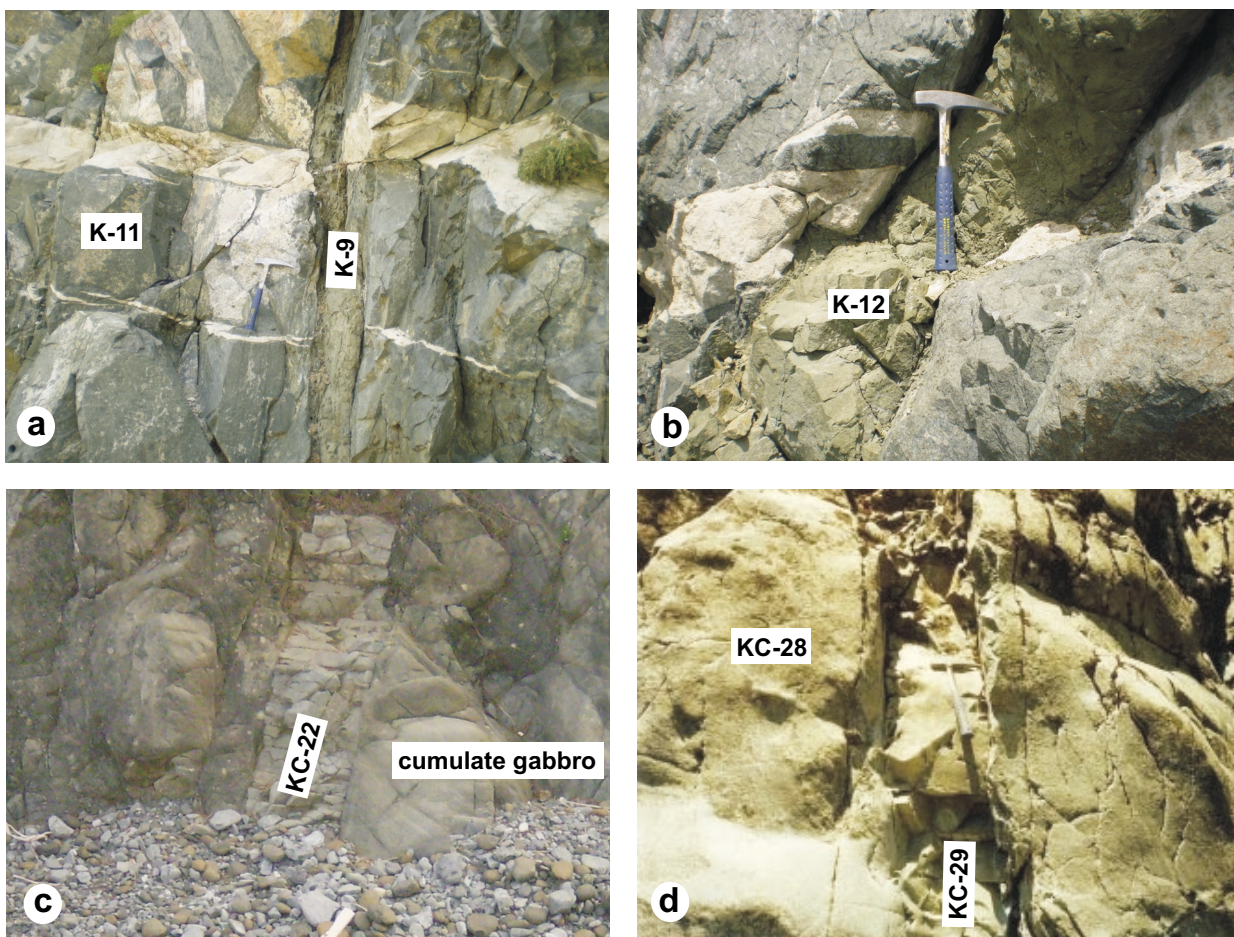


Figure 13. Cross-cutting relations between (a, b) plagiogranite and sheeted dykes, (c) dykes and cumulate gabbro, and (d) dyke and isotropic gabbro from the Kızıldağ (Hatay) ophiolite. Hammer is 33 cm long.

tholeiites (Lower Pillow Lava: Robinson *et al.* 1983; Beccaluva & Serri 1988). This situation seems to be site specific and indicates that distinctly different magma sources were contemporaneously active in a relatively restricted sector across an intraoceanic suprasubduction region. Boninites generally form early in the arc history but are often coincident with and/or follow generation of arc tholeiites (Lytwyn & Casey 1993). This may indicate progressive source depletion from island arc tholeiites to boninites with time.

In conclusion, new geological and geochemical data suggest that (i) the crustal units of the Kızıldağ (Hatay) ophiolite were fed by IAT and boninitic-type magmas and (ii) spatial and temporal relations suggest that these magmas were contemporaneously active in a fore-arc tectonic setting in the southern Neotethys ocean during the Late Cretaceous.

Acknowledgments

This work is a part of PhD study of Utku Bağcı. Financial support from the Çukurova University Research Foundation (Project No: FBE2000D12) is gratefully acknowledged. We would like to thank Fabio Capponi for performing major and trace element analyses, and Dan Topa for his guidance during the microprobe analysis at Salzburg University (Austria). We are grateful to Professor Michel Delaloye for thoughtful discussions on the evolution of the eastern Mediterranean ophiolites. Osman Parlak gratefully acknowledges financial support from TÜBA (Turkish Academy of Sciences). Yıldırım Dilek, John Shervais and Erdin Bozkurt are thanked for their constructive and very helpful comments. John A. Winchester helped with the English of the final text.

Table 8. Summary table for the isotropic gabbros.

Sample No	Rock type	Longitude/Latitude	Locality	Geochemical character	Spatial and temporal relations
K-6	Gabbro	35° 54' 45.5" E / 36° 07' 58.9" N	Çevlik, 25 m north of Güverçinkayası burnu	IAT type	Cut by boninitic dyke (KC-7)
KC-30	Gabbro	35° 58' 52.2" E / 36° 11' 36.7" N	Karaçay valley	IAT type	
KC-34	Quartz diorite	35° 58' 52.2" E / 36° 11' 36.7" N	Karaçay valley	IAT type	
KC-35	Quartz diorite	35° 58' 52.2" E / 36° 11' 36.7" N	Karaçay valley	IAT type	
KC-36	Diorite	35° 58' 51.3" E / 36° 11' 40.0" N	Karaçay valley	IAT type	Cut by IAT-type dyke (KC-37)
KC-39	Quartz diorite	35° 58' 43.6" E / 36° 11' 48.3" N	Karaçay valley	IAT type	
KC-41	Diorite	35° 58' 37.8" E / 36° 11' 53.3" N	Karaçay valley	IAT type	
KC-46	Quartz diorite	35° 58' 47.2" E / 36° 11' 57.9" N	Karaçay valley	IAT type	Cut by IAT-type dyke (KC-47)
T-6	Diorite	35° 54' 37.0" E / 36° 12' 30.9" N	Tazi yurdu (Bakacak Tepé)	IAT type	
U-6	Diorite	35° 43' 51.9" E / 36° 18' 56.8" N	Üçgedik	IAT type	
U-7	Diorite	35° 43' 52.9" E / 36° 18' 55.9" N	Üçgedik	IAT type	Cut by IAT-type dyke (U-8)
K-8	Gabbro	35° 54' 21.4" E / 36° 8' 37.7" N	Çevlik, Karmuşun kayası	Boninitic-type	
K-27	Gabbro	35° 52' 41.9" E / 36° 10' 41.7" N	Çevlik, Ambardere	Boninitic-type	
K-28	Diorite	35° 52' 51.2" E / 36° 10' 22.9" N	Çevlik, Hırlavuk burnu	Boninitic-type	
KC-28	Gabbro	35° 58' 52.9" E / 36° 11' 32.2" N	Karaçay valley	Boninitic-type	
KC-32	Diorite	35° 58' 52.2" E / 36° 11' 36.7" N	Karaçay valley	Boninitic-type	
KC-33	Gabbro	35° 58' 52.2" E / 36° 11' 36.7" N	Karaçay valley	Boninitic-type	
KC-38	Diorite	35° 58' 46.7" E / 36° 11' 44.9" N	Karaçay valley	Boninitic-type	
KC-40	Gabbro	35° 58' 39.7" E / 36° 11' 51.6" N	Karaçay valley	Boninitic-type	
KC-44	Gabbro	35° 58' 26.9" E / 36° 11' 57.6" N	Karaçay valley	Boninitic-type	
KC-45	Gabbro	35° 58' 26.9" E / 36° 11' 57.6" N	Karaçay valley	Boninitic-type	
KC-48	Diorite	35° 58' 21.1" E / 36° 12' 3.5" N	Karaçay valley	Boninitic-type	Cut by boninitic dyke (KC-49)

Table 9. Summary table for the sheeted dykes.

Sample No	Rock type	Longitude/Latitude	Locality	Geochemical character	Spatial and temporal relations
AK-15	Diabase	35° 58' 26.9" E / 36° 11' 57.6" N	Aydinli	IAT type	
K-5	Diabase	35° 54' 50.8" E / 36° 7' 54.8" N	Çevlik	IAT type	
K-11	Diabase	35° 54' 45.6" E / 36° 7' 48.4" N	Güvercinkayası burnu	IAT type	Cut by plagiogranite
K-13	Diabase	35° 54' 1.8"E / 36° 9' 16.3" N	Değirmendere (Çevlik)	IAT type	
K-14	Diabase	35° 53' 49.4" E / 36° 9' 32.0" N	Çevlik	IAT type	
K-30	Diabase	35° 53' 23.4" E / 36° 10' 0.2" N	Çevlik	IAT type	
KÇ-29	Diabase	35° 58' 53.0" E / 36° 11' 32.2" N	Karacay	IAT type	Cutting the boninitic type isotropic gabbro (KC-28)
KÇ-31	Diabase	35° 58' 52.2" E / 36° 11' 36.7" N	Karacay valley	IAT type	
KÇ-37	Diabase	35° 58' 51.3" E / 36° 11' 40.0" N	Karacay valley	IAT type	Cutting the IAT-type isotropic gabbro (KC-36)
KÇ-47	Diabase	35° 58' 24.0" E / 36° 11' 58.5" N	Karacay valley	IAT type	
KÇ-51	Diabase	35° 58' 21.1" E / 36° 12' 3.5" N	Karacay valley	IAT type	Cut by IAT-type dyke (KC-52)
KÇ-52	Diabase	35° 58' 21.1" E / 36° 12' 3.5" N	Karacay valley	IAT type	Cutting the IAT-type dyke (KC-51)
T-11	Diabase	35° 55' 58.9" E / 36° 11' 32.1" N	Tazi yurdu	IAT type	
U-8	Quartz microdiorite	35° 43' 52.9" E / 36° 18' 55.9" N	Ürgedik	IAT type	Cutting the IAT-type isotropic gabbro (U-7)
U-9	Diabase	35° 43' 54.8" E / 36° 18' 52.6" N	Ürgedik	IAT type	
K-4	Diabase	35° 54' 50.8" E / 36° 7' 54.8" N	Çevlik	Boninitic-type	
K-7	Diabase	35° 54' 43.3" E / 36° 8' 8.7" N	Çevlik	Boninitic-type	Cutting the IAT type isotropic gabbro (K-6)
K-9	Diabase	35° 54' 45.6" E / 36° 7' 48.4" N	Çevlik, Güvercinkayası burnu	Boninitic-type	Cutting the plagiogranite
K-12	Diabase	35° 54' 45.6" E / 36° 7' 48.4" N	Çevlik, Güvercinkayası burnu	Boninitic-type	Cutting the plagiogranite
K-25A	Diabase	35° 52' 28.3" E / 36° 10' 51.8" N	Çevlik, Şahanlık kayası burnu	Boninitic-type	
K-29	Diabase	35° 53' 4.3" E / 36° 10' 51.7" N	Çevlik	Boninitic-type	
K-33	Diabase	35° 52' 28.3" E / 36° 10' 51.8" N	Çevlik	Boninitic-type	
KÇ-22	Diabase	35° 59' 7.9" E / 36° 11' 29.0" N	Karacay valley	Boninitic-type	Cutting the mafic cumulates
KÇ-25	Diabase	35° 59' 5.8" E / 36° 11' 29.1" N	Karacay valley	Boninitic-type	Cutting the mafic cumulates
KÇ-43	Diabase	35° 58' 30.9" E / 36° 11' 56.7" N	Karacay valley	Boninitic-type	Cutting the boninitic type isotropic gabbro (KC-48)
KÇ-49	Diabase	35° 58' 21.1" E / 36° 12' 3.5" N	Karacay valley	Boninitic-type	
T-10	Diabase	35° 55' 58.9" E / 36° 11' 32.1" N	Tazi yurdu	Boninitic-type	

Table 10. Summary table for the sakalavites.

Sample No	Rock type	Longitude/Latitude	Locality
SKL-1	Hyaloclastite	36° 10' 49,5" E / 36° 10' 22,3" N	Altunözü road section
SKL-2	Pillow lava	36° 10' 49,5" E / 36° 10' 22,3" N	Altunözü road section
SKL-3	Pillow lava	36° 10' 49,1" E / 36° 10' 22,1" N	Altunözü road section
SKL-4	Hyaloclastite	36° 10' 49,7" E / 36° 10' 21,4" N	Altunözü road section
SKL-5	Pillow lava	36° 10' 49,7" E / 36° 10' 21,4" N	Altunözü road section
SKL-6	Hyaloclastite	36° 10' 50,6" E / 36° 10' 20,8" N	Altunözü road section
SKL-7	Pillow lava	36° 10' 51,2" E / 36° 10' 20,8" N	Altunözü road section
SKL-8	Pillow lava	36° 10' 51,8" E / 36° 10' 20,1" N	Altunözü road section
SKL-9	Hyaloclastite	36° 10' 52,2" E / 36° 10' 19,5" N	Altunözü road section
SKL-10	Pillow lava	36° 10' 52,2" E / 36° 10' 19,0" N	Altunözü road section
SKL-11	Hyaloclastite	36° 10' 53,0" E / 36° 10' 18,3" N	Altunözü road section
SKL-12	Hyaloclastite	36° 10' 53,0" E / 36° 10' 18,3" N	Altunözü road section
SKL-13	Hyaloclastite	36° 10' 52,6" E / 36° 10' 17,6" N	Altunözü road section
SKL-14	Pillow lava	36° 10' 52,8" E / 36° 10' 17,2" N	Altunözü road section
SKL-15	Hyaloclastite	36° 10' 53,0" E / 36° 10' 17,1" N	Altunözü road section
SKL-16	Pillow lava	36° 10' 53,4" E / 36° 10' 16,9" N	Altunözü road section
SKL-17	Hyaloclastite	36° 10' 53,5" E / 36° 10' 16,5" N	Altunözü road section
SKL-18	Pillow lava	36° 10' 54,0" E / 36° 10' 14,6" N	Altunözü road section

References

- ALABASTER, T., PEARCE, J.A. & MALPAS, J. 1982. The volcanic stratigraphy and petrogenesis of the Oman ophiolite complex. *Contributions to Mineralogy and Petrology* **81**, 168–183.
- AL-RIYAMI, K., ROBERTSON, A.H.F., DIXON, J. & XENOPHONTOS, C. 2002. Origin and emplacement of the Late Cretaceous Baer-Bassit ophiolite and its metamorphic sole in NW Syria. *Lithos* **65**, 225–260.
- ARCUS, R.J. & POWELL, R. 1986. Source component mixing in the regions of arc magma generation. *Journal of Geophysical Research* **91**, 5913–5926.
- ARCUS, R.J., PEARCE, J.A., MURTON, B.J. & VAN DER LAAN, S.R. 1992. Igneous stratigraphy and major element geochemistry of holes 786A and 786B. *Proceeding of Ocean Drilling Program Scientific Results* **125**, 143–169.
- BAĞCI, U., PARLAK, O. & HÖCK, V. 2005. Whole rock and mineral chemistry of cumulates from the Kızıldağ (Hatay) ophiolite (Turkey): clues for multiple magma generation during crustal accretion in the southern Neotethyan ocean. *Mineralogical Magazine* **69**, 53–76.
- BAĞCI, U., PARLAK, O. & HÖCK, V. 2006. Geochemical character and tectonic environment of ultramafic to mafic cumulates from the Tekirova (Antalya) ophiolite (southern Turkey). *Geological Journal* **41**, 193–219.
- BAĞCI, U. & PARLAK, O. 2007. Petrology of the Tekirova (Antalya) ophiolite (Southern Turkey): evidence for diverse magma generations and their tectonic implications during Neotethyan subduction. *International Journal of Earth Sciences* [in review].
- BECCALUVA, L. & SERRI, G. 1988. Boninitic and low-Ti subduction-related lavas from intraoceanic arc-backarc systems and low-Ti ophiolites: a reappraisal of their petrogenesis and original tectonic setting. *Tectonophysics* **146**, 291–315.
- BECCALUVA, L., OHNSTETTER, D., OHNSTETTER, M. & PAUPY, A. 1984. Two magmatic series with island arc affinities within the Vourinos ophiolite. *Contributions to Mineralogy and Petrology* **85**, 253–271.
- BECCALUVA, L., COLTORTI, M., GIUNTA, G. & SIENA, F. 2004. Tethyan vs Cordilleran ophiolites: A reappraisal of distinctive tectonomagmatic features of suprasubduction complexes in relation to the subduction mode. *Tectonophysics* **393**, 163–174.
- BECCALUVA, L., COLTORTI, M., SACCANI, E. & SIENA, F. 2005. Magma generation and crustal accretion as evidenced by supra-subduction ophiolites of the Albanide-Hellenide Subpelagonian zone. *The Island Arc* **14**, 551–563.
- BEDARD, J.H. 1999. Petrogenesis of boninites from the Betts Cove ophiolite, Newfoundland, Canada: Identification of subducted source components. *Journal of Petrology* **40**, 1853–1889.

- BEDARD, J.H., LAUZIERE, K., TREMBLAY, A. & SANGSTER, A. 1998. Evidence for forearc seafloor-spreading from the Betts Cove ophiolite, Newfoundland: oceanic crust of boninitic affinity. *Tectonophysics* **284**, 233–245.
- BEYARSLAN, M. & BİNGÖL, A.F. 2000. Petrology of a supra-subduction zone ophiolite (Elazığ, Turkey). *Canadian Journal of Earth Sciences* **37**, 1411–1424.
- BLOOMER, S.H. & HAWKINS, J.W. 1983. Gabbroic and ultramafic rocks from the Mariana trench: an island arc ophiolite. In: HAYES, D.E. (ed), *The Tectonic and Geologic Evolution of Southeast Asian Seas*. 2. American Geophysical Union, Washington, D.C., 294–317.
- BLOOMER, S.H. & HAWKINS, J.W. 1983. Petrology and geochemistry of boninite series volcanic rocks from the Mariana trench. *Contributions to Mineralogy and Petrology* **97**, 550–553.
- CAMERON, W.E., NISBET, E.G. & DIETRICH, V.J. 1979. Boninites, komatiites and ophiolitic basalts. *Nature* **280**, 550–553.
- CAWTHORN, R.G. & DAVIES, G. 1983. Experimental data at 3 kbar pressure on parental magma to the Bushveld complex. *Contributions to Mineralogy and Petrology* **83**, 128–135.
- COLEMAN, R.G. 1981. Tectonic setting for ophiolite obduction in Oman. *Journal of Geophysical Research* **86**, 2497–2508.
- CRAWFORD, A.J. 1989. *Boninites*. Unwin Hyman, London.
- CRAWFORD, A.J., FALLOON, T.J. & GREEN, D.H. 1989. Classification, petrogenesis and tectonic setting of boninites. In: CRAWFORD, A.J. (ed.), *Boninites and Related Rocks*. Unwin Hyman Ltd, UK, 1–49.
- DELALOYE, M. & WAGNER, J.J. 1984. Ophiolites and volcanic activity near the western edge of the Arabian plate. In: DIXON, J.E. & ROBERTSON, A.H.F. (eds), *The Geological Evolution of the Eastern Mediterranean*. Geological Society, London, Special Publications **17**, 225–233..
- DILEK, Y. 2003. Ophiolite concept and its evolution. In: DILEK, Y. & NEWCOMB, S. (eds), *Ophiolite Concept and the Evolution of Geological Thought*. The Geological Society of America, Special Paper **373**, 1–16.
- DILEK, Y. & DELALOYE, M. 1992. Structure of the Kızıldağ ophiolite, a slow-spread Cretaceous ridge segment north of the Arabian promontory. *Geology* **20**, 19–22.
- DILEK, Y. & EDDY, C.A. 1992. The Troodos (Cyprus) and the Kızıldağ (S. Turkey) ophiolites as structural models for slow-spreading ridge segments. *Journal of Geology* **100**, 305–322.
- DILEK, Y. & FLOWER, M.F.J. 2003. Arc-trench rollback and forearc accretion: 2. A model template for ophiolites in Albania, Cyprus, and Oman. In: DILEK, Y. & ROBINSON, P.T. (eds), *Ophiolites in Earth History*. Geological Society, London, Special Publications **218**, 43–68.
- DILEK, Y. & THY, P. 1998. Structure, petrology and seafloor spreading tectonics of the Kızıldağ ophiolite, Turkey. In: MILLS, R.A. & HARRISON, K. (eds), *Modern Ocean Floor Processes and the Geological Record*. Geological Society, London, Special Publications **148**, 43–69..
- DILEK, Y., THY, P., MOORES, E.M. & RAMSDEN, T.W. 1990. Tectonic evolution of the Troodos ophiolite within the Tethyan framework. *Tectonics* **9**, 811–823.
- DILEK, Y., MOORES, E.M., DELALOYE, M. & KARSON, J.A. 1991. A magmatic extension and tectonic denudation in the Kızıldağ ophiolite, southern Turkey: implications for the evolution of Neotethyan oceanic crust. In: PETERS, T., NICOLAS, A. & COLEMAN, R.G. (eds), *Ophiolite Genesis and Evolution of the Oceanic Lithosphere*. Kluwer Academic Publishers, The Netherlands, 487–502.
- DILEK, Y., THY, P., HACKER, B. & GRUNDVIG, S. 1999. Structure and petrology of Tauride ophiolites and mafic dyke intrusions (Turkey): implications for the Neotethyan ocean. *Bulletin of Geological Society America* **111**, 1192–1216.
- DROOP, G.T.R. 1987. A general equation for estimating Fe⁺³ in ferromagnesian silicates and oxides from microprobe analysis, using stoichiometric criteria. *Mineralogical Magazine* **51**, 431–437.
- DUBERTRET, L. 1955. Géologie des roches vertes du nord-ouest de la Syrie et du Hatay (Turquie). *Notes Mémoires Moyen-Orient* **6**, p. 227.
- ERENDİL, M. 1984. Petrology and structures of the upper crustal units of the Kızıldağ ophiolite. In: TEKELİ, O. & GÖNCÜOĞLU, M.C. (eds), *Proceedings of International Symposium on the Geology of the Tauride Belt*. Mineral Research and Exploration Institute (MTA) of Turkey Publications, Ankara, 269–284.
- FALLOON, T.J. & CRAWFORD, A.J. 1991. The petrogenesis of high-Ca boninite lavas dredged from the northern Tonga ridge. *Earth and Planetary Science Letters* **102**, 375–394.
- FALLOON, T.J., MALAHOFF, A., ZONENSHAIN, L.P. & BOGDANOV, Y. 1992. Petrology and geochemistry of back arc basin basalts from Lau Basin spreading ridges at 15°, 18°, and 19°S. *Mineralogy and Petrology* **47**, 1–35.
- FLOYD, P.A. & WINCHESTER, J.A. 1975. Magma type and tectonic setting discrimination using immobile elements. *Earth and Planetary Science Letters* **27**, 211–218.
- GASS, I.G. & SMEWING, J.D. 1973. Intrusion, extrusion and metamorphism at constructive margins: evidence from the Troodos massif, Cyprus. *Nature* **242**, 26–29.
- GREEN, D.H. 1976. Equilibrium testing of 'equilibrium' partial melting of peridotite under water-saturated, high-pressure conditions. *Canadian Mineralogist* **14**, 255–268.
- HART, S.R., ERLANK, A.J. & KABLE, E.J.D. 1974. Sea floor basalt alteration: some chemical and Sr isotopic effects. *Contributions to Mineralogy and Petrology* **44**, 219–230.
- HAWKINS, J.W., BLOOMER, S.H., EVANS, C.A. & MELCHIOR, J.T. 1984. Evolution of intra-oceanic-arc trench system. *Tectonophysics* **102**, 175–205.
- HICKEY, R. & FREY, F.A. 1982. Geochemical characteristics of boninite series volcanics: implications for their source. *Geochimica et Cosmochimica Acta* **46**, 2099–2115.

- HUMPRIS, S.E. & THOMPSON, G. 1978. Trace element mobility during hydrothermal alteration of oceanic basalts. *Geochimica et Cosmochimica Acta* **42**, 127–136.
- JAKES, P. & GILL, J. 1970. Rare earth elements and the island arc tholeiitic series. *Earth and Planetary Science Letters* **9**, 17–28.
- JENNER, G.A. 1981. Geochemistry of high-Mg andesites from Cape Vogel, Papua New Guinea. *Chemical Geology* **33**, 307–332.
- JENNER, G.A. 1983. *Petrogenesis of High-Mg Andesites: An Experimental and Geochemical Study With Emphasis on High-Mg Andesites From Cape Vogel, PNG*. PhD Thesis, University of Tasmania, Hobart [unpublished].
- LAURENT, R., DELALOYE, M., VAUGNAT, M. & WAGNER, J.J. 1980. Composition of parental basaltic magma in ophiolites. In: PANAYIOTOU, A. (ed), *Proceedings of International Ophiolite Symposium*. Geological Survey Department, Cyprus, 172–181.
- LIPPARD, S.J., SHELTON, A.W. & GASS, I.G. 1986. The ophiolite of Northern Oman. *Geological Society, London, Memoir* **11**.
- LIVERMORE, R.A. & SMITH, A.G. 1984. Some boundary conditions for the evolution of the Mediterranean Region. In: STANLEY, D.J. & WEZEL, F.C. (eds), *Geological Evolution of the Mediterranean Basin*. Springer-Verlag, Berlin, 83–100.
- LYTWYN, J.N. & CASEY, J.F. 1993. Geochemistry and petrogenesis of volcanics and sheeted dikes from the Hatay (Kızıldağ) ophiolite, southern Turkey: possible formation with the Troodos ophiolite, Cyprus, along fore-arc spreading centers. *Tectonophysics* **223**, 237–272.
- MALPAS, J. & LANGDON, G. 1984. Petrology of upper pillow lava suite, Troodos ophiolite, Cyprus. In: GASS, I.G., LIPPARD, S.J. & SHELTON, A.W. (eds) Geological Society, London, Special Publications **13**, 155–167.
- MALPAS, J., MOORES, E.M. & PANAYIOTOU, A. 1990. *Ophiolites, Oceanic Crustal Analogues*. Geological Survey Department, Cyprus, Nicosia.
- MEFFRE, S., AITCHISON, J. & CRAWFORD, A.J. 1996. Geochemical evolution and tectonic significance of boninites and tholeiites from the Koh ophiolite, New Caledonia. *Tectonics* **15**, 67–83.
- MEIJER, A. 1980. Primitive arc series volcanism and a boninitic series: examples from western Pacific island arc. *American Geophysical Union Monographs* **23**, 269–282.
- MEIJER, A., ANTHONY, E. & REAGEN, M. 1980. Petrology of volcanic rocks from the fore-arc sites. *Initial Reports on Deep Sea Drilling Projects* **60**, 709–724.
- MOORES, E.M. & VINE, F.J. 1971. Troodos Massif, Cyprus and other ophiolites as oceanic crust: evaluation and implications. *Philosophical Transactions of the Royal Society, London* **A268**, 443–466.
- MUKASA, S.B. & LUDDEN, J.N. 1987. Uranium-lead ages of plagiogranites from the Troodos ophiolite, Cyprus, and their tectonic significance. *Geology* **15**, 825–828.
- MURTON, B.J. 1989. Tectonic controls on boninite genesis. In: SAUNDERS, A.D. & NORRY, M.J. (eds), *Magmatism in the Ocean Basins*. Geological Society, London, Special Publications **42**, 347–377.
- NICOLAS, A. 1989. *Structure of Ophiolites and Dynamics of Oceanic Lithosphere*. Kluwer Academic Publisher, The Netherlands.
- PANAYIOTOU, A. 1980. *Ophiolites, Proceedings of the International Ophiolite Symposium, Cyprus, 1979*. Geological Survey Department Cyprus, Nicosia.
- PARLAK, O. 1996. *Geochemistry and Geochronology of the Mersin Ophiolite within the Eastern Mediterranean Tectonic Frame*. PhD Thesis, University of Geneva, Switzerland, Terre & Environnement **6**.
- PARLAK, O. 2006. Petrology of Neotethyan ophiolites in Turkey: Distinct magma generations and their tectonic significance. *Mesozoic Ophiolite Belts of Northern Part of the Balkan Peninsula. International Ophiolite Symposium*, Belgrade-Banja Luka, 106–109.
- PARLAK, O., DELALOYE, M. & BİNGÖL, E. 1996. Mineral chemistry of the arc-related ultramafic-mafic cumulates as an indicator of the arc-related origin of the Mersin ophiolite (southern Turkey). *Geologische Rundschau* **85**, 647–661.
- PARLAK, O., DELALOYE, M. & HÖCK, V. 2000. Suprasubduction zone origin of the Pozanti-Karsanti ophiolite (southern Turkey) deduced from whole-rock and mineral chemistry of the gabbroic cumulates. In: BOZKURT, E., WINCHESTER, J.A. & PIPER, J.D.A. (eds), *Tectonics and Magmatism in Turkey and the Surrounding Area*. Geological Society, London, Special Publications **173**, 219–234.
- PARLAK, O., HÖCK, V. & DELALOYE, M. 2002. The supra-subduction zone Pozanti-Karsanti ophiolite, Southern Turkey: evidence for high-pressure crystal fractionation of ultramafic cumulates. *Lithos* **65**, 205–224.
- PARLAK, O., HÖCK, V., KOZLU, H. & DELALOYE, M. 2004. Oceanic crust generation in an island arc tectonic setting, SE Anatolian Orogenic Belt (Turkey). *Geological Magazine* **141**, 583–603.
- PEARCE, J.A. 1982. Trace element characteristics of lavas from destructive plate boundaries. In: THORPE, R.S. (ed), *Andesites*. Wiley and Sons, New York, 525–548.
- PEARCE, J.A. 1983. Role of the sub-continental lithosphere in magma genesis at active continental margins. In: HAWKESWORTH, C.J. & NORRY, M.J. (eds), *Continental Basalts and Mantle Xenoliths*. Shiva, Nantwich, 230–249.
- PEARCE, J.A. 1996. A users guide to basalt discrimination diagrams. In: Wyman, D.A. (ed), *Trace Element Geochemistry of Volcanic Rocks: Applications for Massive Sulphide Exploration*. Geochemistry Short Course Notes, Geological Association of Canada, 79–113.
- PEARCE, J.A. 2003. Supra-subduction zone ophiolites: The search for modern analogues. In: DILEK, Y. & NEWCOMB, S. (eds), *Ophiolite Concept and the Evolution of Geological Thought*. Geological Society of America, Special Paper **373**, 269–293.
- PEARCE, J.A. & CANN, J.R. 1973. Tectonic setting of basaltic volcanic rocks determined using trace element analysis. *Earth and Planetary Science Letters* **19**, 290–300.

- PEARCE, J.A. & NORRY, M.J. 1979. Petrogenetic implications of Ti, Zr, Y, and Nb variations in volcanic rocks. *Contributions to Mineralogy and Petrology* **69**, 33–47.
- PEARCE, J.A., LIPPARD, S.J. & ROBERTS, S. 1984. Characteristics and tectonic significance of suprasubduction zone ophiolites. In: KOKELAAR, B.P. & HOWELLS, M.F. (eds), *Marginal Basin Geology*. Geological Society, London, Special Publications **16**, 77–94.
- PE-PIPER, G., TSIKOURAS, B. & HATZIPANAGIOTOU, K. 2004. Evolution of boninites and island-arc tholeiites in the Pindos ophiolite, Greece. *Geological Magazine* **141**, 455–469.
- PİŞKİN, Ö., DELALOYE, M., MORITZ, R. & WAGNER, J.J. 1990. Geochemistry and geothermometry of the Hatay complex Turkey: implication for genesis of the ophiolite sequence. In: MALPAS, J., MOORES, E.M., PANAYIOTOU, A. & XENOPHONTOS, C. (eds), *Proceeding of Troodos Ophiolite Symposium*. Geological Survey Department, Cyprus, 329–337.
- REAGAN, M.K. & MEIJER, A. 1984. Geology and geochemistry of early arc-volcanic rocks from Guam. *Bulletin of Geological Society of America* **95**, 701–713.
- RIZAOĞLU, T., PARLAK, O., HöCK, V. & İŞLER, F. 2006. Nature and significance of Late Cretaceous ophiolitic rocks and its relation to the Baskil granitoid in Elazığ region, SE Turkey. In: ROBERTSON, A.H.F. & MOUNTRAKIS, D. (eds), *Tectonic Development of the Eastern Mediterranean Region*. Geological Society, London, Special Publications **260**, 327–350.
- ROBERTSON, A.H.F. 1986a. The Hatay ophiolite (Southern Turkey) in its eastern Mediterranean tectonic context: a report on some aspects of the field excursion. *Ophioliti* **11**, 105–119.
- ROBERTSON, A.H.F. 1986b. Geochemistry and tectonic implications of metalliferous and volcanoclastic sedimentary rocks associated with late cretaceous ophiolitic extrusives in the Hatay area, southern Turkey. *Ophioliti* **11**, 121–140.
- ROBERTSON, A.H.F. 1998. Mesozoic-Tertiary tectonic evolution of the easternmost Mediterranean area: integration of marine and land evidence. In: ROBERTSON A.H.F., EMEIS, K.C., RICHTER, C. & CAMERLENGHI, A. (eds), *Proceedings of the Ocean Drilling Program, Scientific Results* **160**, 723–782.
- ROBERTSON, A.H.F. 2000. Mesozoic-Tertiary tectonic-sedimentary evolution of a south Tethyan oceanic basin and its margins in southern Turkey. In: BOZKURT, E., WINCHESTER, J.A. & PIPER, J.D. (eds), *Tectonics and Magmatism in Turkey and Surrounding Area*. Geological Society, London, Special Publications **173**, 43–82.
- ROBERTSON, A.H.F. 2002. Overview of the genesis and emplacement of Mesozoic ophiolites in the Eastern Mediterranean Tethyan region. *Lithos* **65**, 1–67.
- ROBINSON, P.T., MELSON, W.G., O'HEARN, T. & SCHMINCKE, H.U. 1983. Volcanic glass compositions of the Troodos ophiolite, Cyprus. *Geology* **11**, 400–404.
- SACCANI, E. & PHOTIADES, A. 2004. Mid-ocean ridge and supra-subduction affinities in the Pindos Massif ophiolites (Greece): implications for magma genesis in a proto-forearc setting. *Lithos* **73**, 229–253.
- SACCANI, E. & PHOTIADES, A. 2005. Petrogenesis and tectonomagmatic significance of volcanic and subvolcanic rocks in the Albanide-Hellenide ophiolitic mélange. *The Island Arc* **14**, 494–516.
- SAVOSTIN, L.A., SIBUET, J.C., ZONENSHAIN, L.P., LE PICHON, X. & ROLET, J. 1986. Kinematic evolution of the Tethys belt, from the Atlantic to the Pamirs since the Triassic. *Tectonophysics* **123**, 1–35.
- SELÇUK, H. 1981. *Etude géologique de la partie méridionale du Hatay (Turquie)*. These Doctora, Université de Genève, Suisse [unpublished].
- SHERVAIS, J.W. 1982. Ti-V plots and the petrogenesis of modern ophiolitic lavas. *Earth and Planetary Science Letters* **59**, 101–118.
- SMELLIE, J.L., STONE, P. & EVANS, J. 1995. Petrogenesis of boninites in the Ordovician Ballantrae Complex ophiolite, southwestern Scotland. *Journal of Volcanology and Geothermal Research* **69**, 323–342.
- STERN, R.J. & BLOOMER, S.H. 1992. Subduction zone infancy: examples from the Eocene Izu-Bonin-Mariana and Jurassic California arcs. *Bulletin of Geological Society of America* **104**, 1621–1636.
- SUN, S.S. & McDONOUGH, W.F. 1989. Chemical and isotopic systematics of ocean basalts: Implications for mantle composition and processes. In: SAUNDERS, A.D. & NORRY, M.J. (eds), *Magmatism in the Ocean Basins*. Geological Society, London, Special Publications **42**, 313–346.
- SENGÖR, A.M.C. & YILMAZ, Y. 1981. Tethyan evolution of Turkey: a plate tectonic approach. *Tectonophysics* **75**, 181–241.
- TATSUMI, Y. 1982. Origin of high-magnesian andesites in the Setouchi volcanic belt, southwest Japan, II. Melting phase relations at high-pressure. *Earth and Planetary Science Letters* **60**, 305–317.
- TAYLOR, R.N. & NESBITT, R.W. 1994. Arc volcanism in an extensional regime at the initiation of subduction—a geochemical study of Hahajima, Bonin Island, Japan. In: SMELLIE, J.L. (ed), *Volcanism Associated With Extension at Consuming Plate Margin*. Geological Society, London, Special Publications **81**, 115–134.
- TEKELİ, O. & ERENİDLİ, M. 1984. Kızıldağ ofiyolitinin (Hatay) jeolojisi ve petrolojisi [Geology and Petrology of the Kızıldağ (Hatay) ophiolite]. *Mineral Research and Exploration Institute (MTA) of Turkey Bulletin* **107**, 33–49 [in Turkish with English abstract].
- TEKELİ, O. & ERENİDLİ, M. 1986. Geology and petrology of the Kızıldağ ophiolite (Hatay). *Mineral Research and Exploration Institute (MTA) of Turkey Bulletin* **21**, 21–37.
- TEKELİ, O., WHITECHURCH, H. & ERENİDLİ, M. 1983. *The Kızıldağ Ophiolite: Autochthons, Para-autochthons and Ophiolites of the Eastern Taurus and Amanos Mountains*. Excursion Guide. International Symposium on the Geology of the Taurus Belt, Ankara, Turkey.
- TINKLER, C., WAGNER, J.J., DELALOYE, M. & SELÇUK, H. 1981. Tectonic history of the Hatay ophiolites (south Turkey) and their interpretation with the Dead Sea rift. *Tectonophysics* **72**, 23–41.
- WALKER, D.A. & CAMERON, W.E. 1983. Boninite primary magmas: evidence from the Cape Vogel peninsula. *Contributions to Mineralogy and Petrology* **83**, 150–158.

- WALLIN, E.T. & METCALF, R.V. 1998. Supra-subduction zone ophiolites formed in an extensional forearc: Trinity terrane, Klamath mountains, California. *Journal of Geology* **106**, 591–608.
- WESSEL, J.K., FRYER, P., WESSEL, P. & TAYLOR, B. 1994. Extension in the Northern Mariana Inner Forearc. *Journal of Geophysical Research* **99**, 15181–15203.
- WINCHESTER, J.A. & FLOYD, P.A. 1977. Geochemical discrimination of different magma series and their differentiation products using immobile elements. *Chemical Geology* **20**, 325–343.
- WOOD, D.A., JORON, J.L. & TREUIL, M. 1979. A reappraisal of the use of trace elements to classify and discriminate between magma series erupted in different tectonic settings. *Earth and Planetary Science Letters* **45**, 326–36.
- WOOD, D.A., MARSH, N.G., TARNEY, J.L., FRYER, P. & TREUIL, M. 1982. Geochemistry of igneous rocks recovered from a transect across the Mariana Trough, arc, fore-arc, and trench, sites 453 though 461, Deep Sea Drilling Project Leg 60. *Initial Reports on Deep Sea Drilling Project* **60**, 709–730.
- WOOD, D.A., MARSH, N.G., TARNEY, J.L., FRYER, P. & TREUIL, M. 1981. Geochemistry of igneous rocks recovered from a transect across the Mariana Trough, arc, forearc, and trench, sites 453 through 461, Deep Sea Drilling Project Leg 60. *Initial Reports on Deep Sea Drilling Project* **60**, 611–645.
- YALINIZ, K.M., FLOYD, P.A. & GÖNCÜOĞLU, M.C. 1996. Supra-subduction zone ophiolites of Central Anatolia: geochemical evidence from the Sarıkaraman ophiolite, Aksaray, Turkey. *Mineralogical Magazin* **60**, 697–710.
- YOGODZINSKI, G.M., VOLYNETS, O.N., KOLOSKOV, A.V., SELIVERSTOV, N.I. & MATVENKOV, V.V. 1993. Magnesian andesites and the subduction component in strongly calc-alkaline series at Piip volcano, far western Aleutians. *Journal of Petrology* **35**, 163–204.

Received 03 September 2006; revised typescript received 10 April 2007; accepted 26 April 2007